

COMPARATIVE ANALYSIS OF DATA FROM NEUTRON AND MUON DETECTORS AT ANTARCTICA

KLEDSAI POOPAKUN

STUDENT ID : 630555916 ASTRONOMY PROGRAM

WHAT ARE COSMIC RAYS ?

- High Energy particles or γ -rays from space
- sources of cosmic rays :
 - from solar winds, solar storms \rightarrow solar energetic particles
 - from supernova explosions inside the Galaxy \rightarrow galactic cosmic rays
 - from gamma-ray bursts (GRBs), AGN outside the Galaxy \rightarrow extragalactic cosmic rays

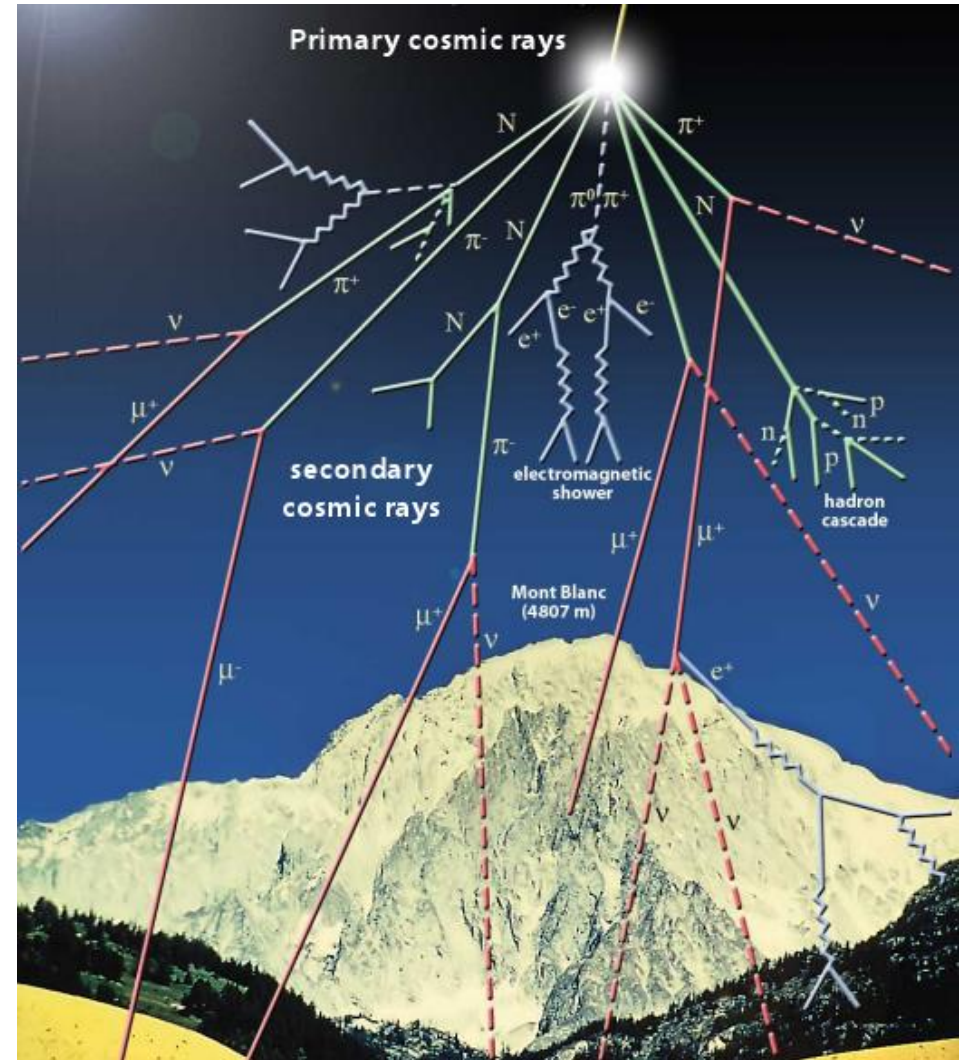
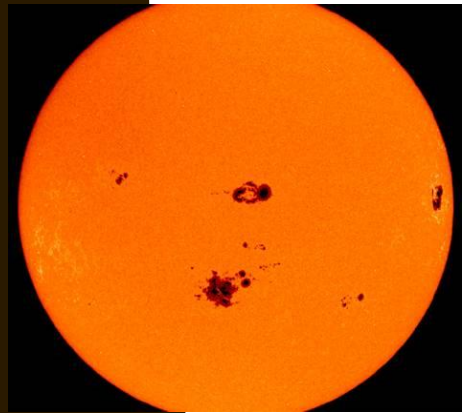


Fig 1. Schematic diagram of a cosmic ray air shower. (Credit: CERN)

SOLAR MODULATION



Credit: NASA

Credit: NASA/GSFC/PFSS

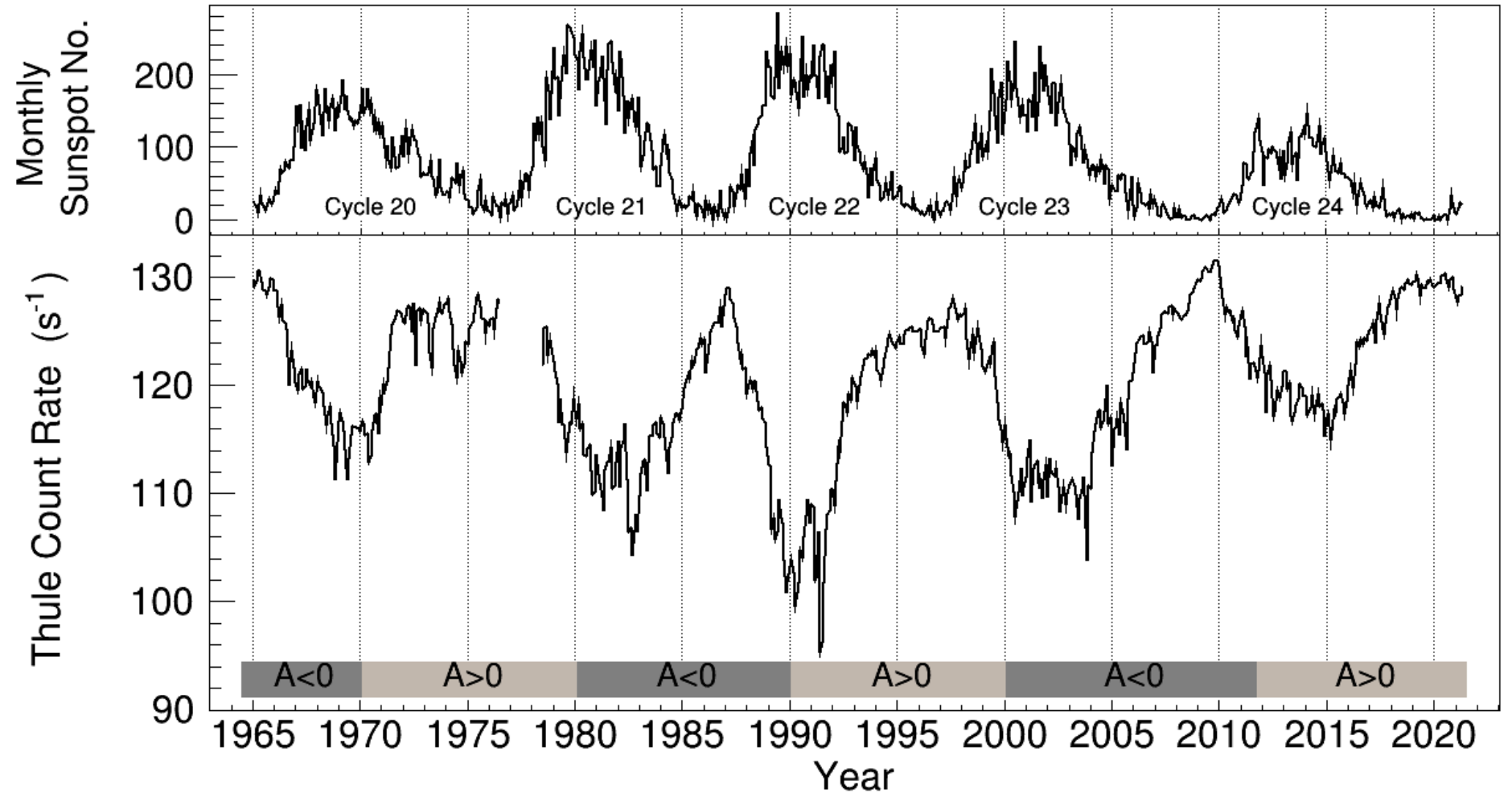
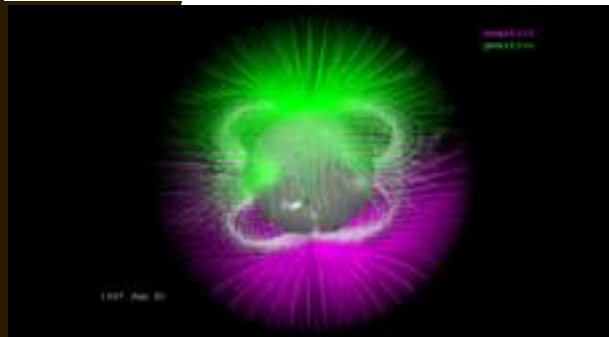


Fig 2. Solar modulation : As solar activity rises (top panel, Source:WDC-SILSO Royal Observatory of Belgium, Brussels), the pressure-corrected count rate recorded by the neutron monitor in Thule decreases (bottom panel, Source: Bartol Research Institute, University of Delaware, USA). The solar magnetic polarity reversal can be seen between positive (denoted by $A > 0$) and negative (denoted by $A < 0$)

SHORT-TERM MODULATION

FORBUSH DECREASE

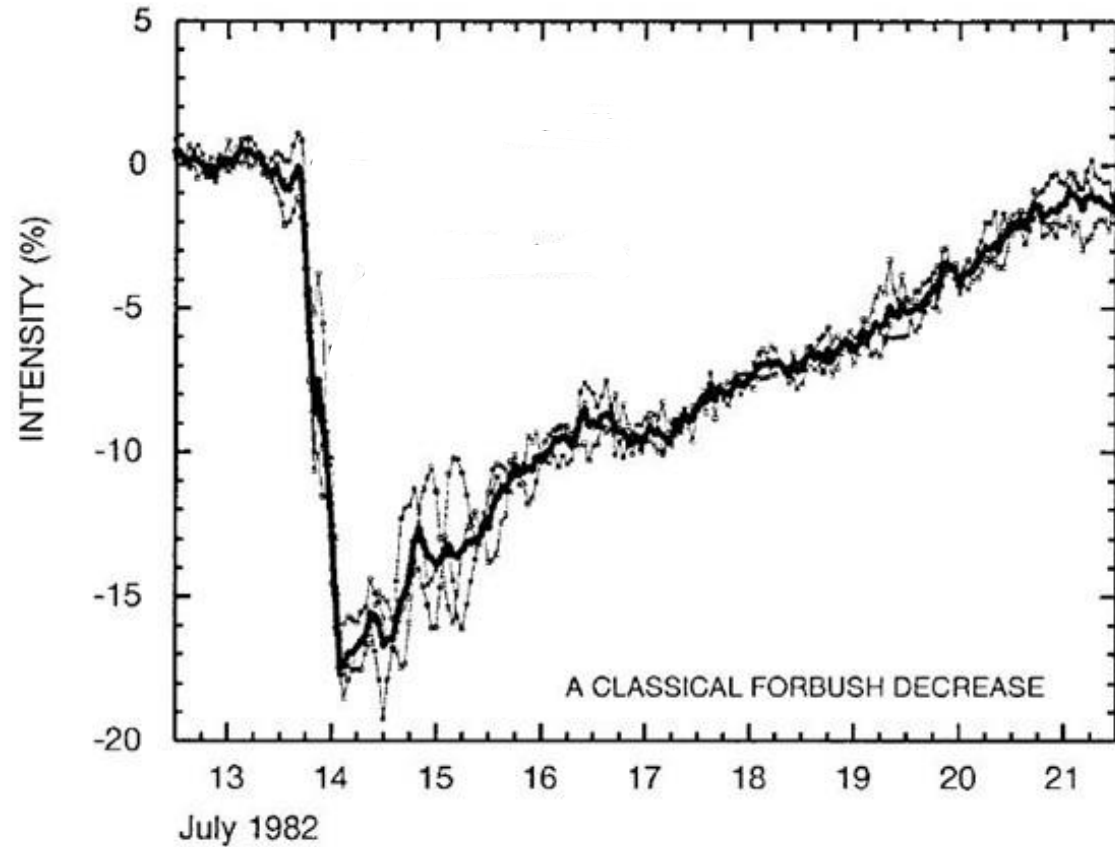


Fig 3. A rapid decrease in the observed galactic cosmic ray intensity

GROUND LEVEL ENHANCEMENT

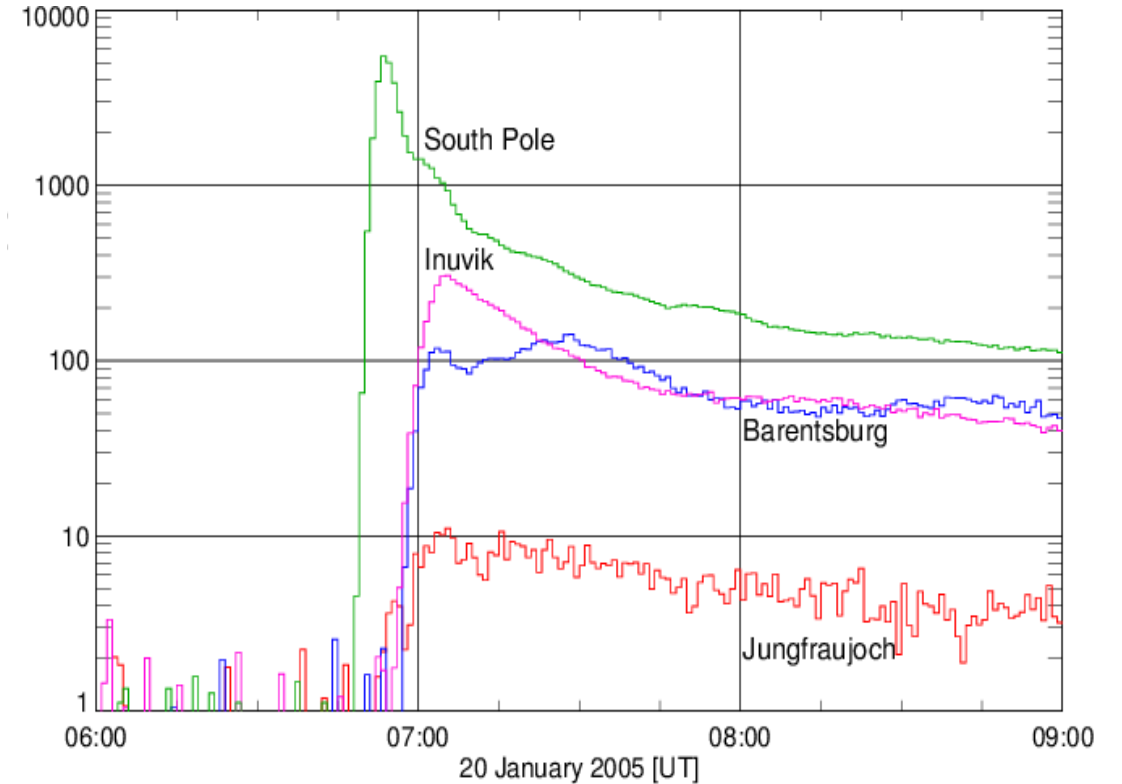


Fig 4. Ground level enhancement onsets at four NM stations recording the event of January 20, 2005 (Flückiger et al., 2005)

CROSSOVER

(Moraal et al., 1989)

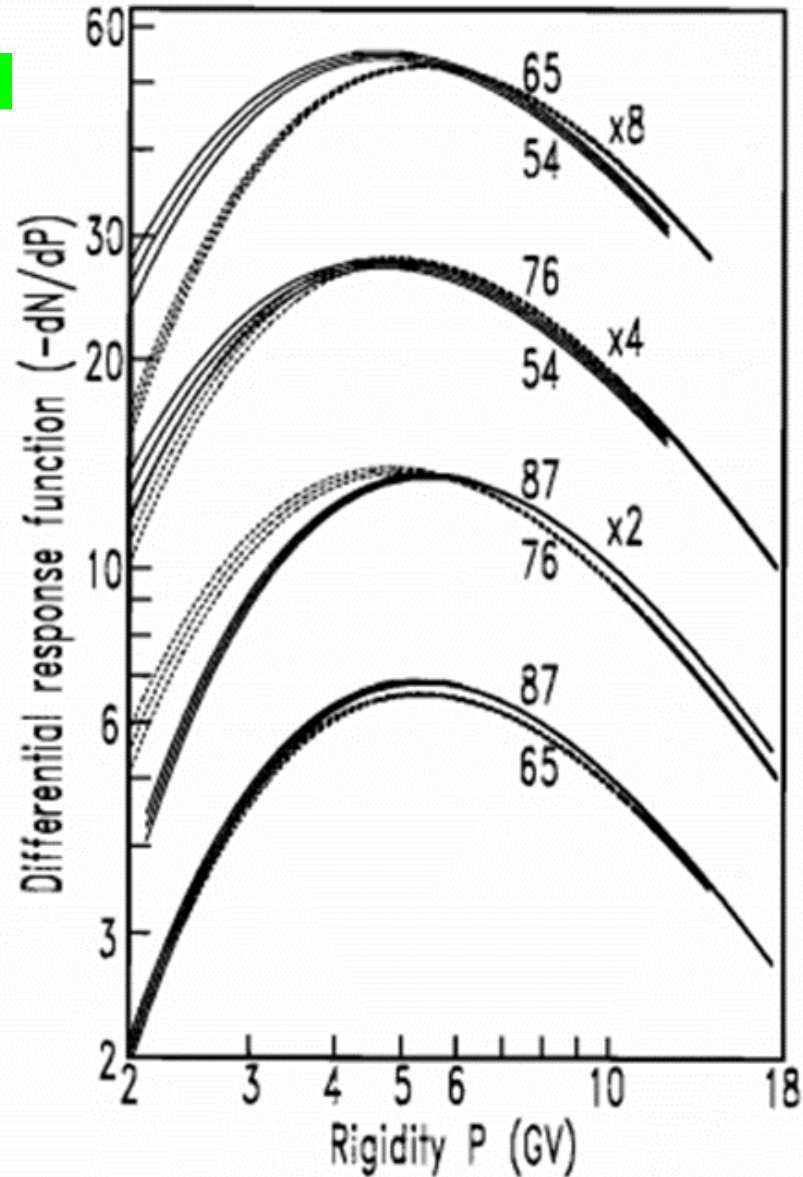


Fig 5. Differential response functions (Moraal et al., 1989)

(Nuntiyakul et al., 2014)

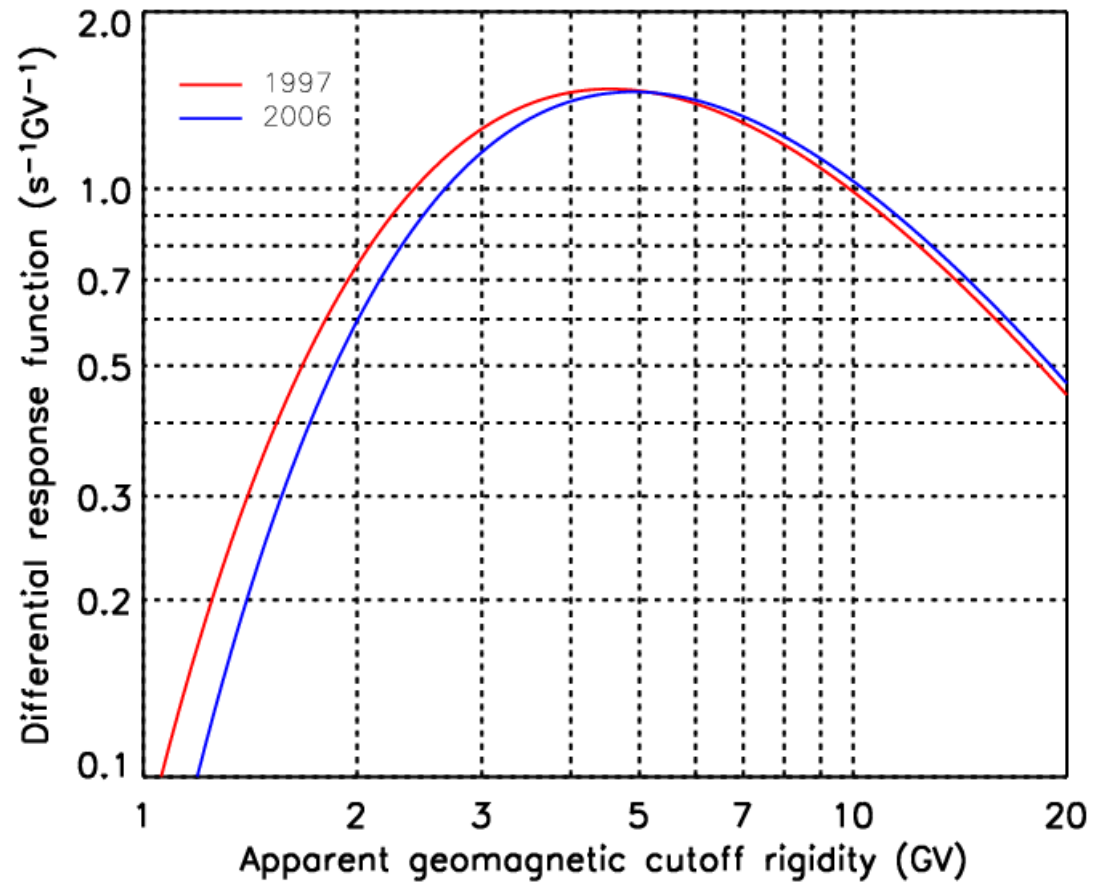
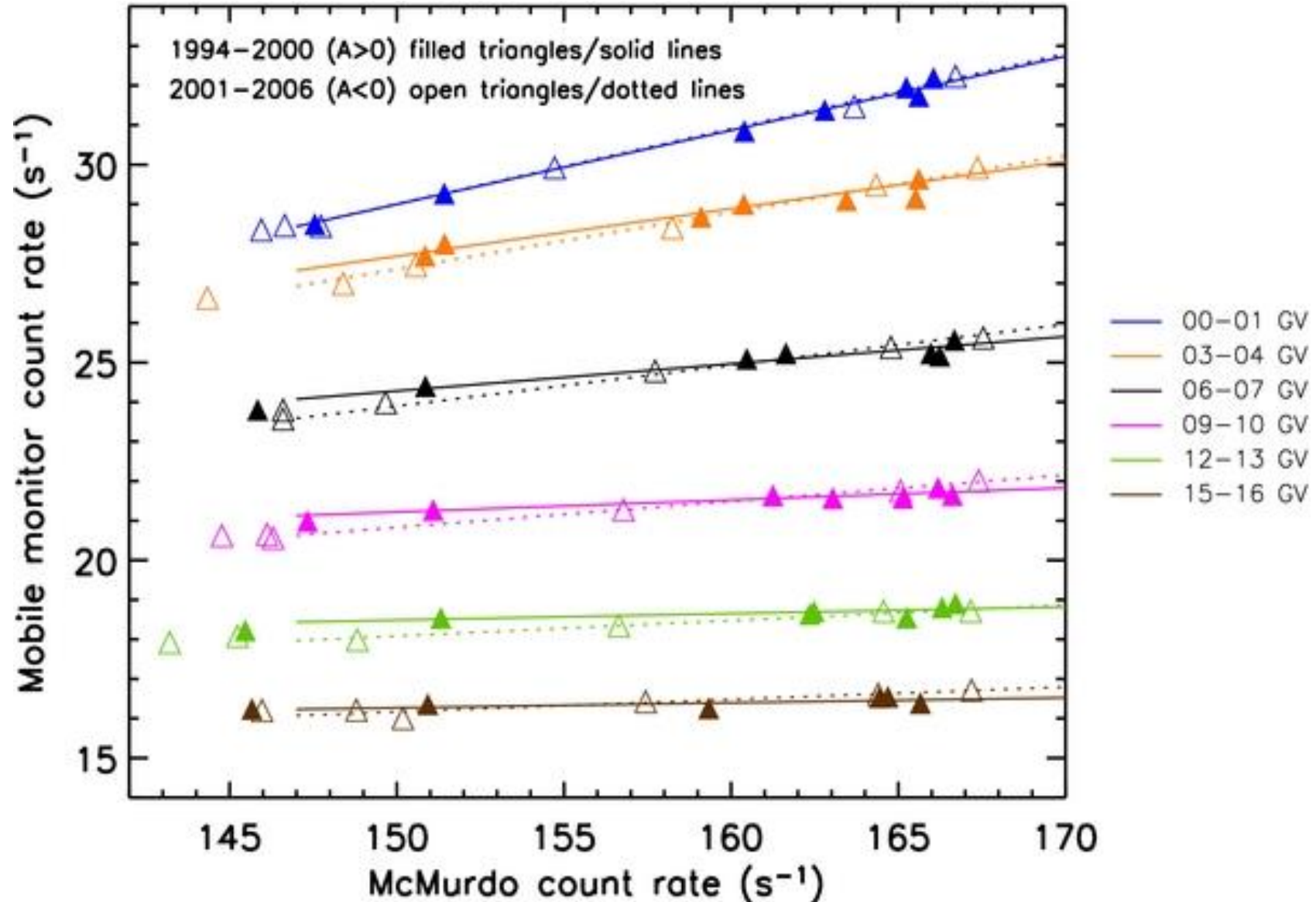


Fig 6. Differential response functions for two survey years, near solar minimum, of opposite polarity and similar modulation level. A crossover is apparent at 4.9 GV. (Nuntiyakul et al., 2014)

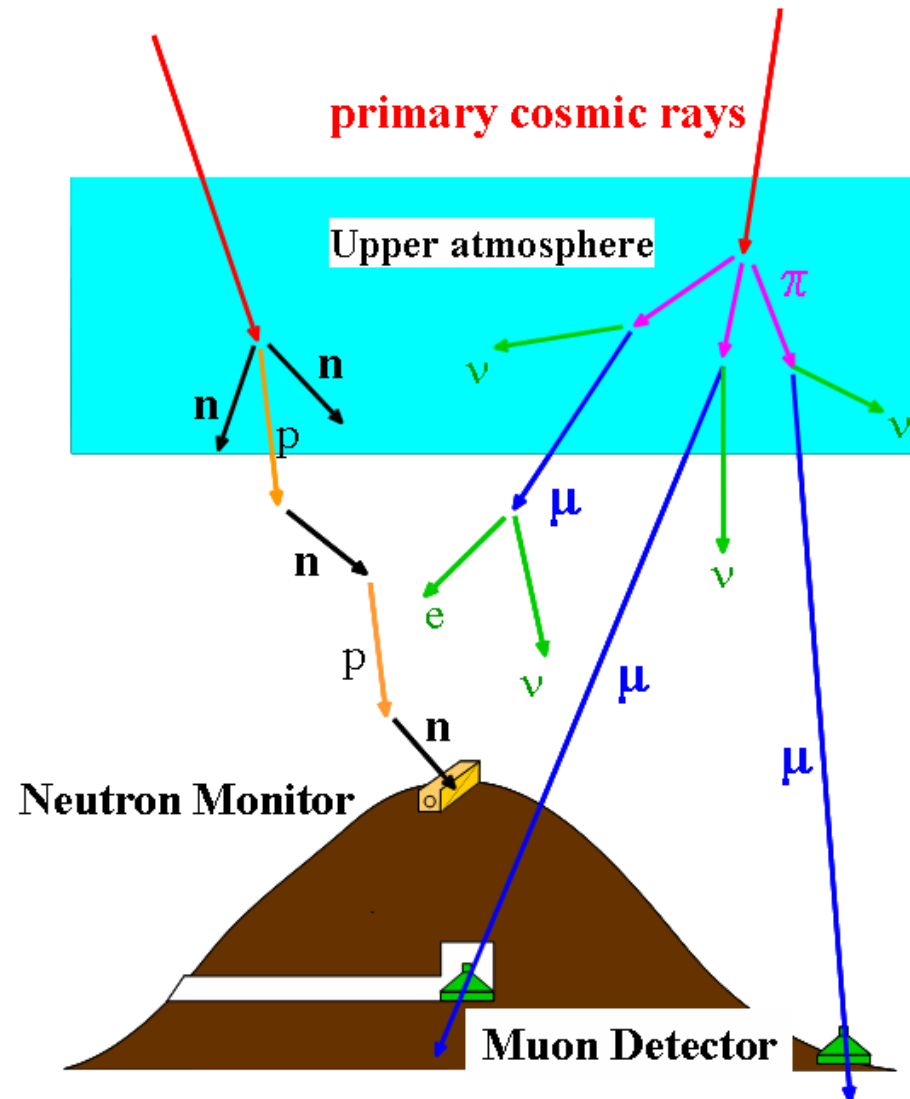
CROSSOVER

Fig 7.

Alternative presentation of the averaged data using selected rigidity bins and superimposing the data for different solar magnetic polarities. A filled triangle is used to indicate positive ($A > 0$) solar magnetic polarity with solid lines showing the linear fits. Open triangles indicate data for negative ($A < 0$) solar magnetic polarity while the dotted lines are linear fits to these data. There are clear differences in cosmic ray modulation before and after the solar magnetic polarity reversal. (Nuntiyakul et al., 2014)



OBSERVATION OF COSMIC RAYS WITH GROUND-BASED DETECTORS



- Ground-based detectors measure byproducts of the interaction of primary cosmic rays with Earth's atmosphere
- Two common types:

Neutron Monitor

Typical energy of primary: ~1 GeV for solar cosmic rays,
~10 GeV for Galactic cosmic rays

Muon Detector

Typical energy of primary: ~50 GeV for Galactic cosmic rays (surface muon detector) and greater for underground muon detector

AIM OF THIS STUDY

- To analyze linear regression of the mobile neutron monitor count rates during the years 1994-2007 and 2018-2020 against Mawson neutron monitor count rates. We are also interested in finding linear regression of the mobile neutron monitor count rate in survey years 2018 and 2019 against Jang Bogo's count rate (installed and operated later in 2016) for comparative purposes with the obtained linear regression against Mawson.
- To use the muon data at Mawson station for different zenith angles to study the spectrum variations.



OBSERVATIONS

LATITUDE SURVEY

Fig 8. 3NM64 installed inside the container for 1994-2007 latitude survey
(Nuntiyakul et al., 2014)

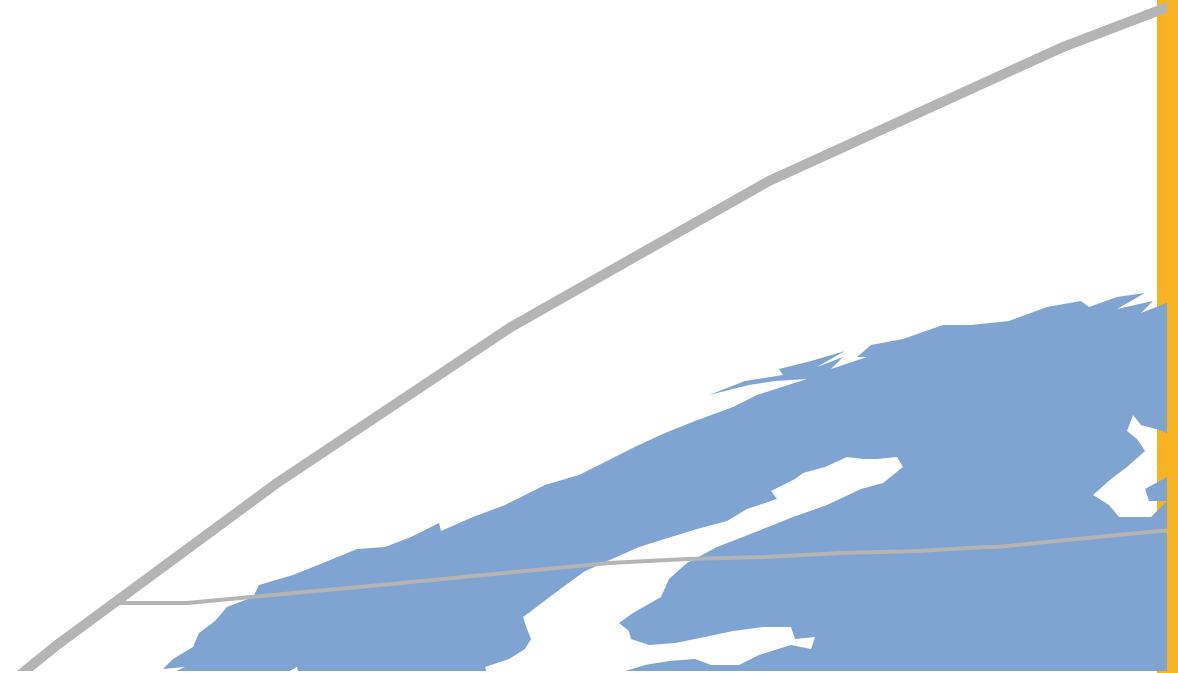


Fig 9 . The track of the ship-borne neutron monitor latitude surveys for 1994-2007 and 2018-2019 superimposed on contours of the vertical cutoff rigidity.

STANDARD NEUTRON MONITOR (NM64)

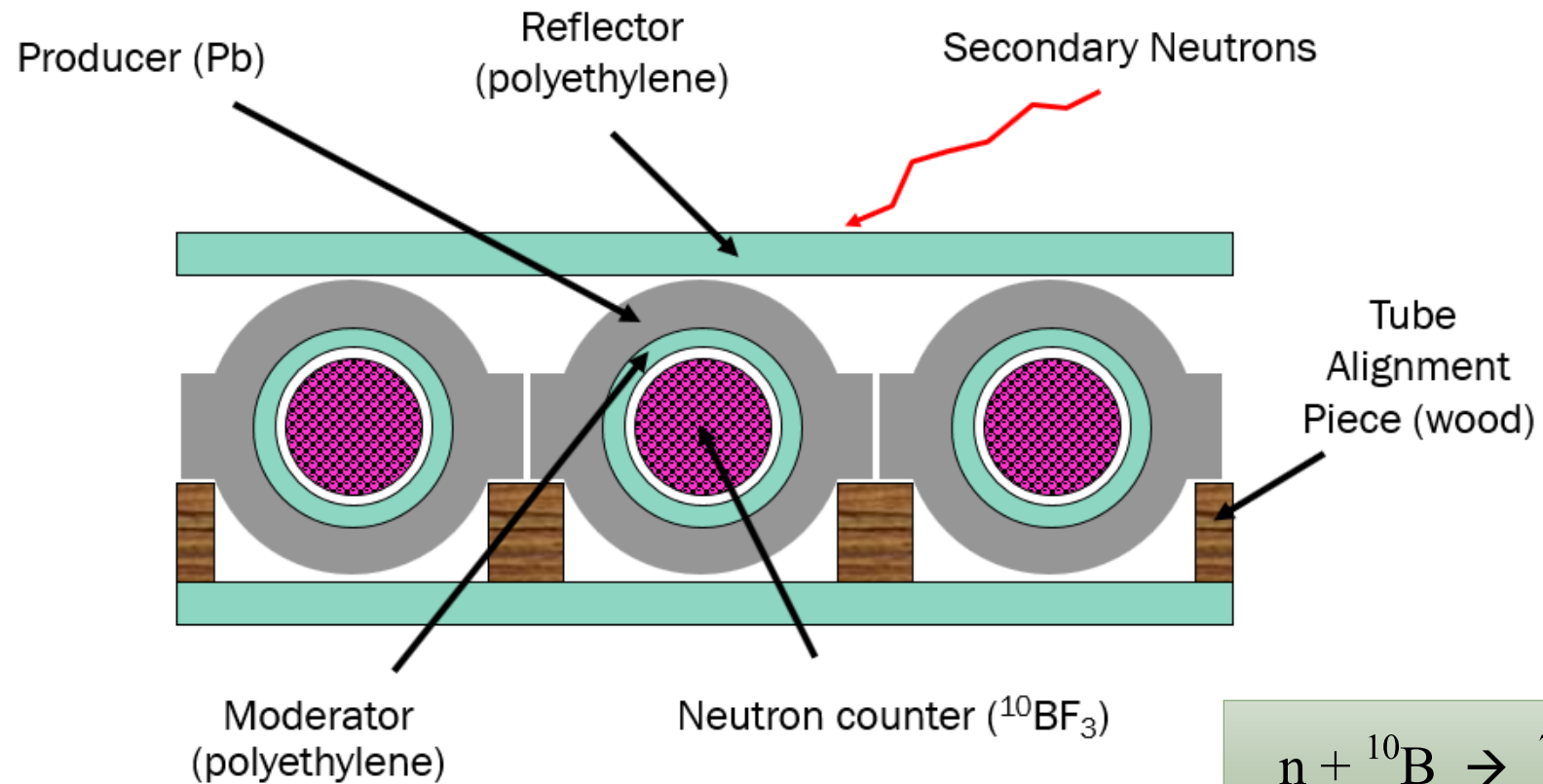


Fig 10. Standard neutron monitor (3NM64)

SAMI-LEADED NEUTRON MONITOR

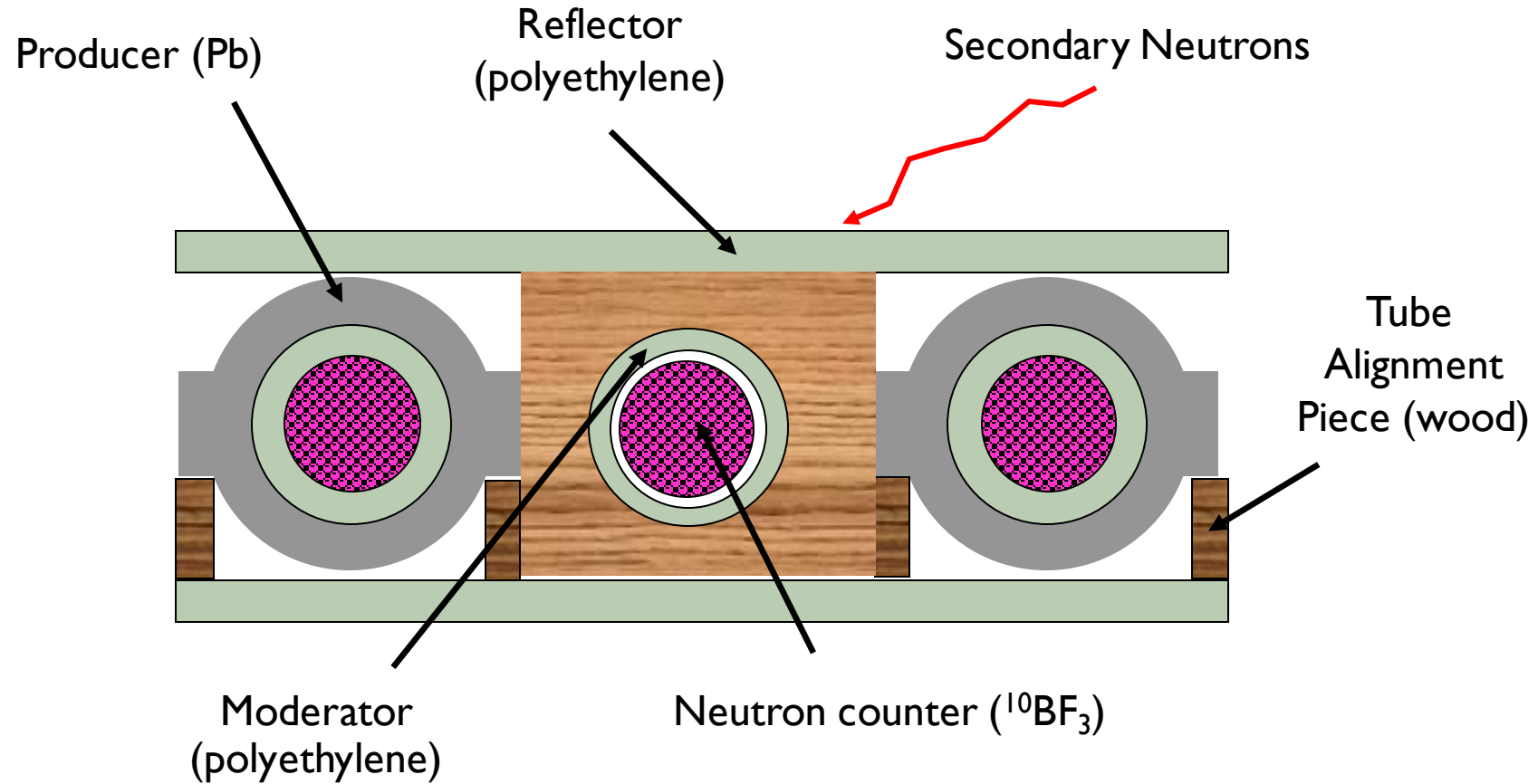
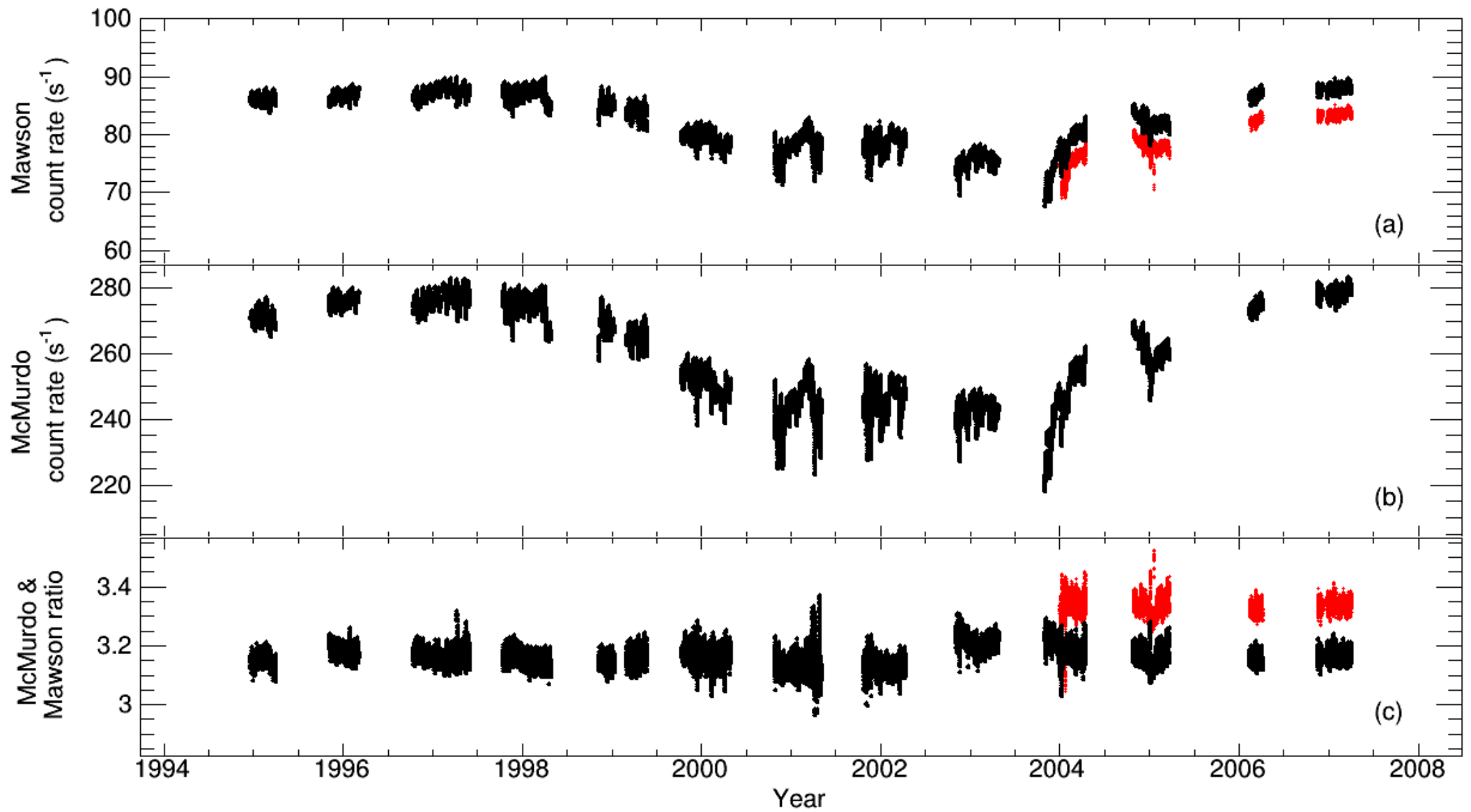
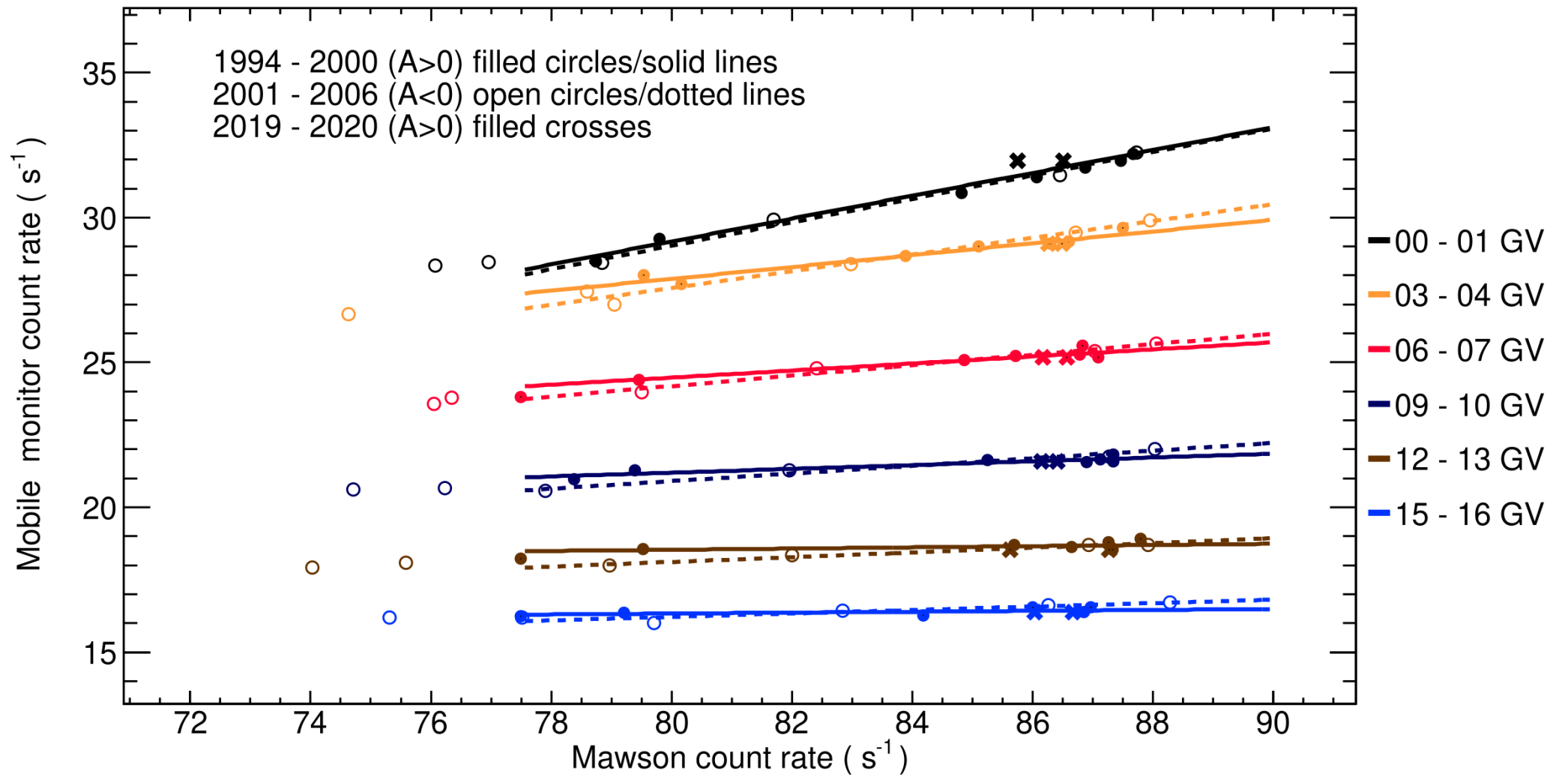


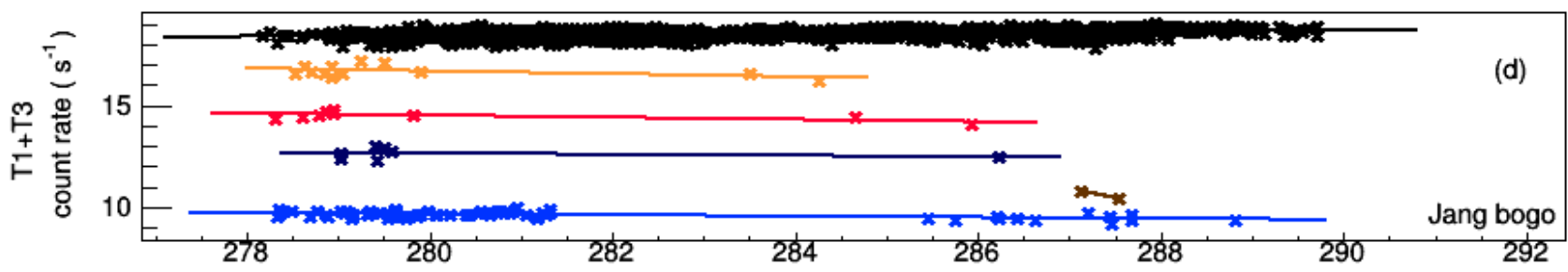
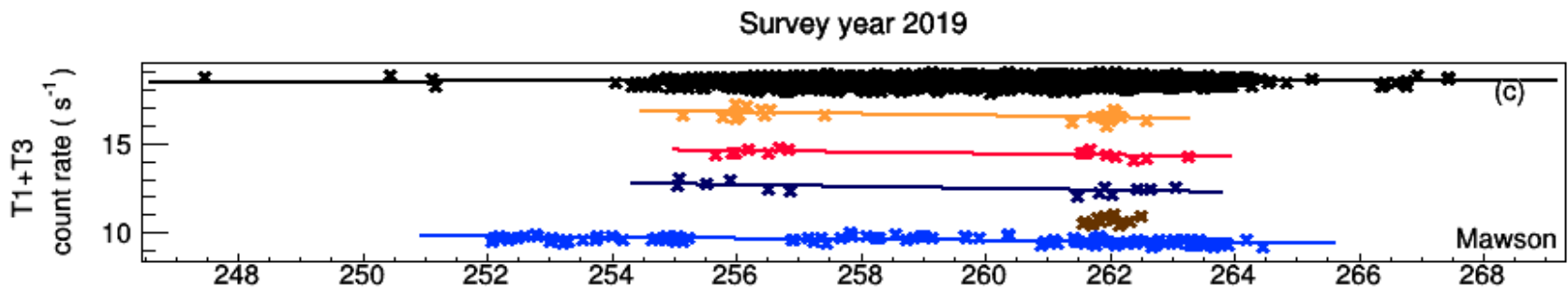
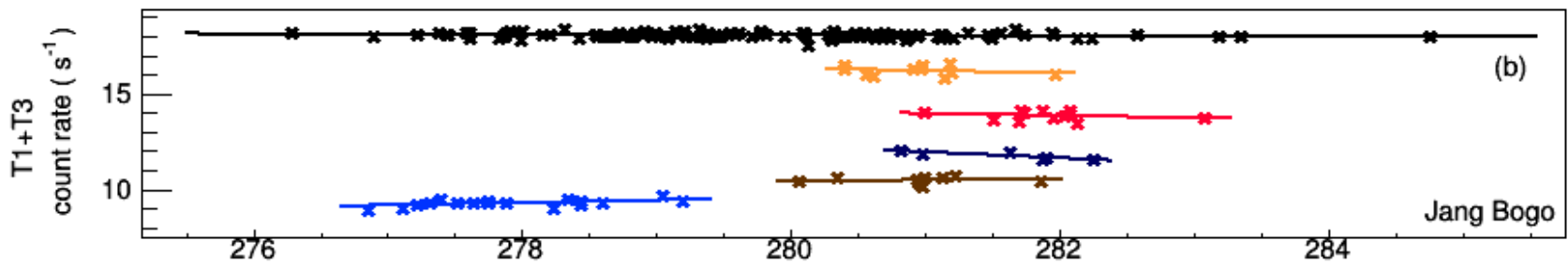
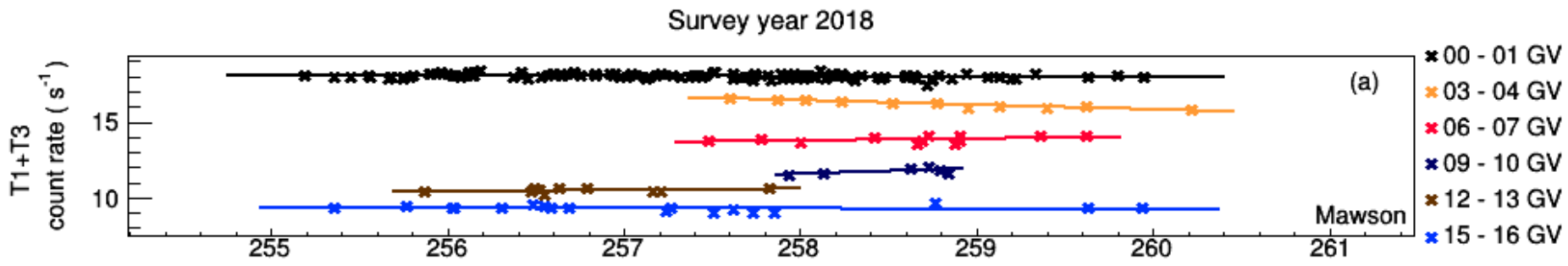
Fig II. Semi-Leaded Neutron Monitor which used for survey year 2018-2019



COMPARE CHANGVAN TO 3NM64

- To compare the two tubes in the recent survey years to the 3NM64 in a 13-year survey, we find multiplicative factors from the ratio of $3NM64_{1997} / (T1+T3)_{2018-2020}$
- We apply a normalization factor of 1.80 for the survey year 2018 and that of 1.75 for the survey year 2019 to T1+T3.





DRF FOR 1997 (+) AND 2006(-)

$$N = N_0(1 - e^{-\alpha P_c^{-\kappa}}),$$

$$N = \int_{P_c}^{\infty} (\text{DRF}) dP$$

$$\text{DRF} = N_0 \alpha P^{-\kappa-1} \kappa (e^{-\alpha P^{-\kappa}}),$$

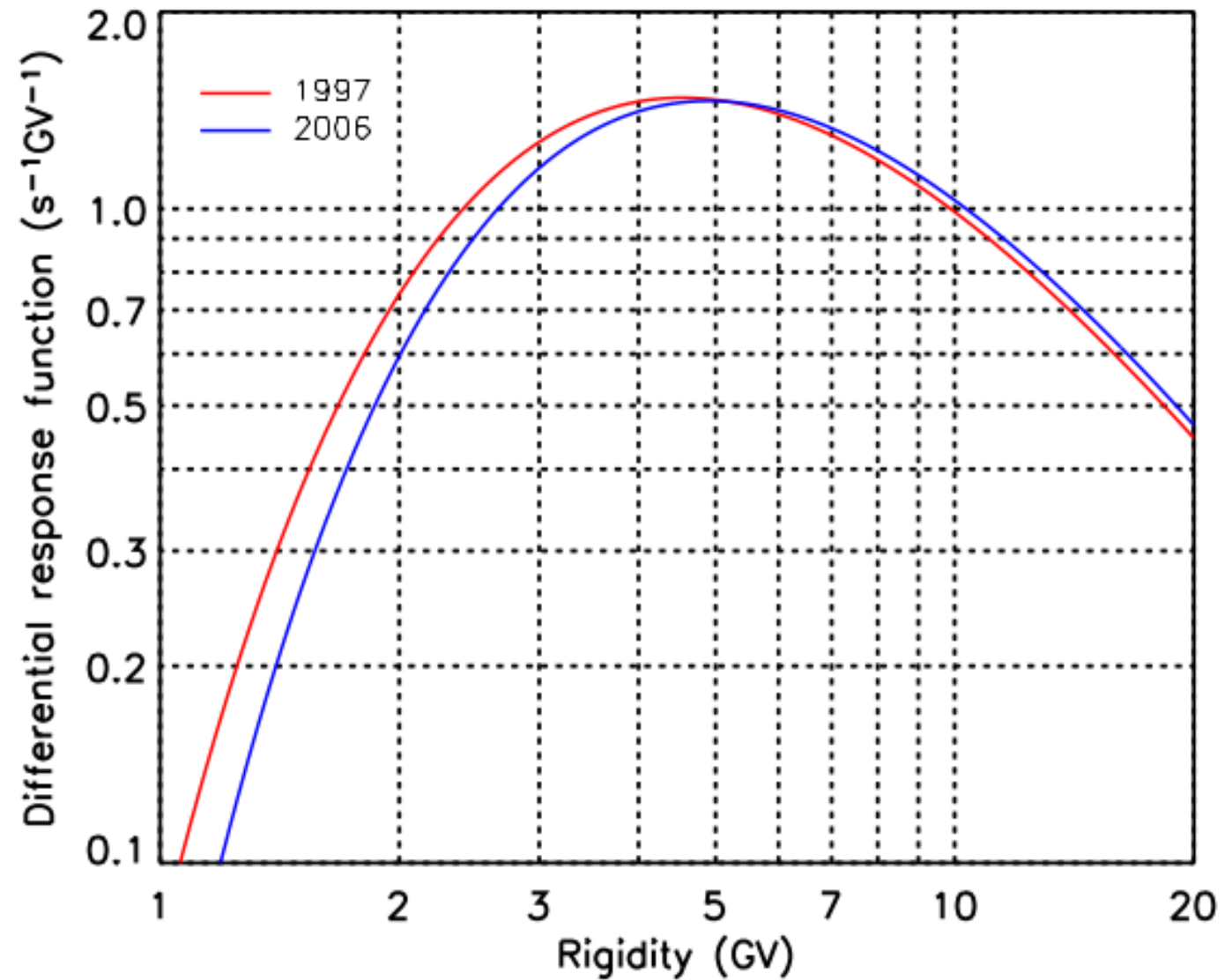
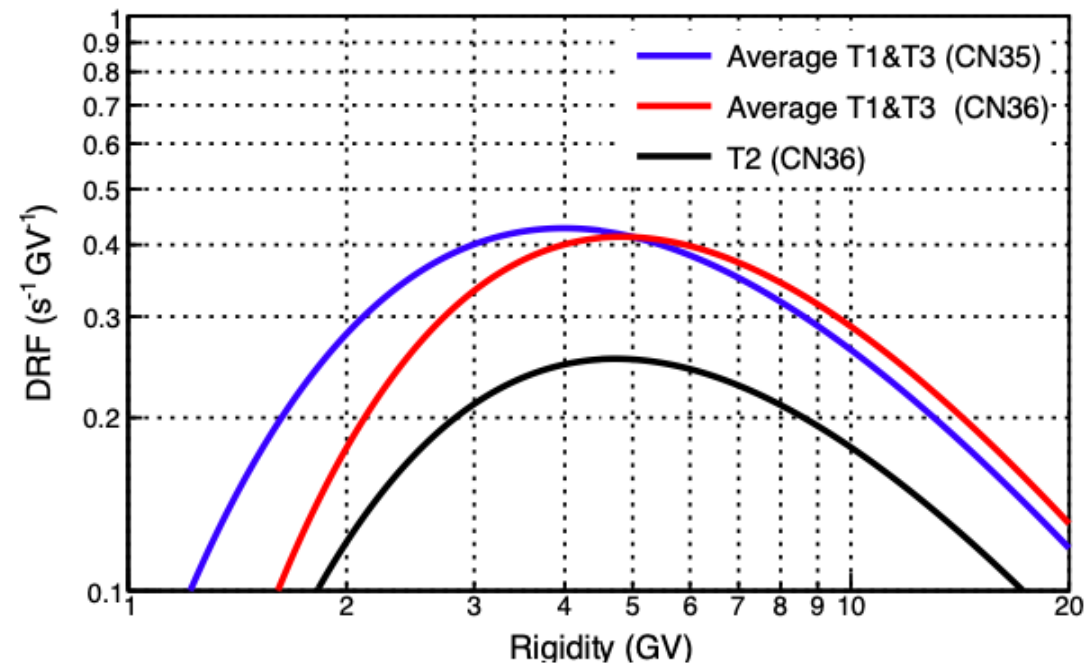
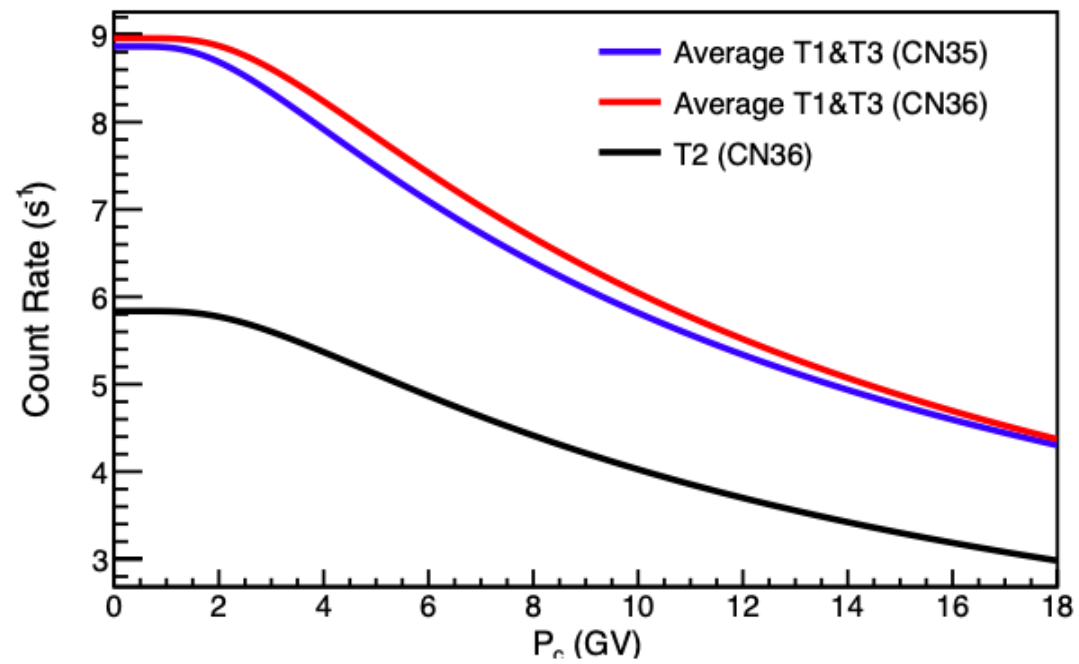


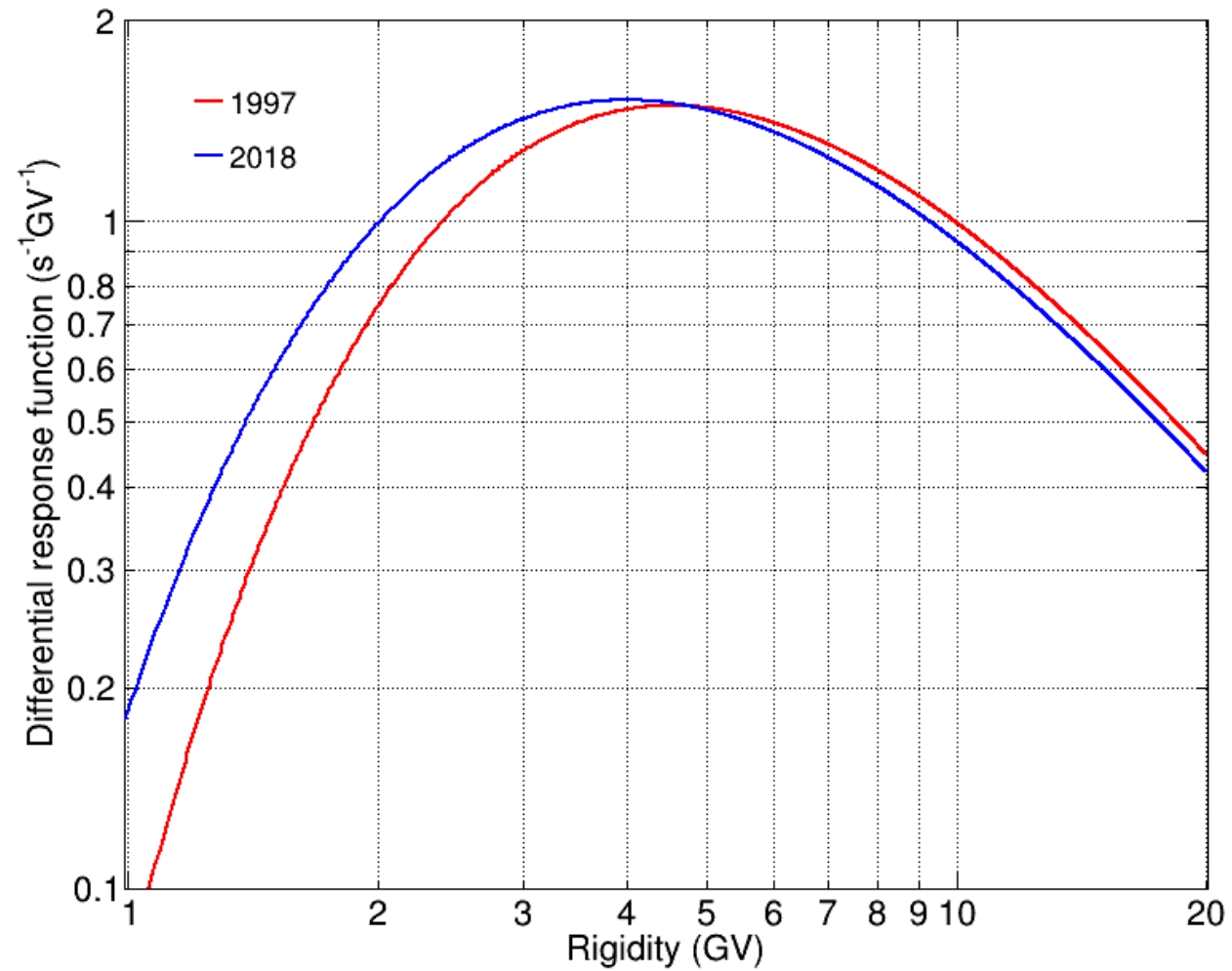
Figure 8. Differential response functions for two survey years, near solar minimum, of opposite polarity and similar modulation level. A crossover is apparent near 5 GV.

Update Dorman Function 2018-2019 (30Nov21)

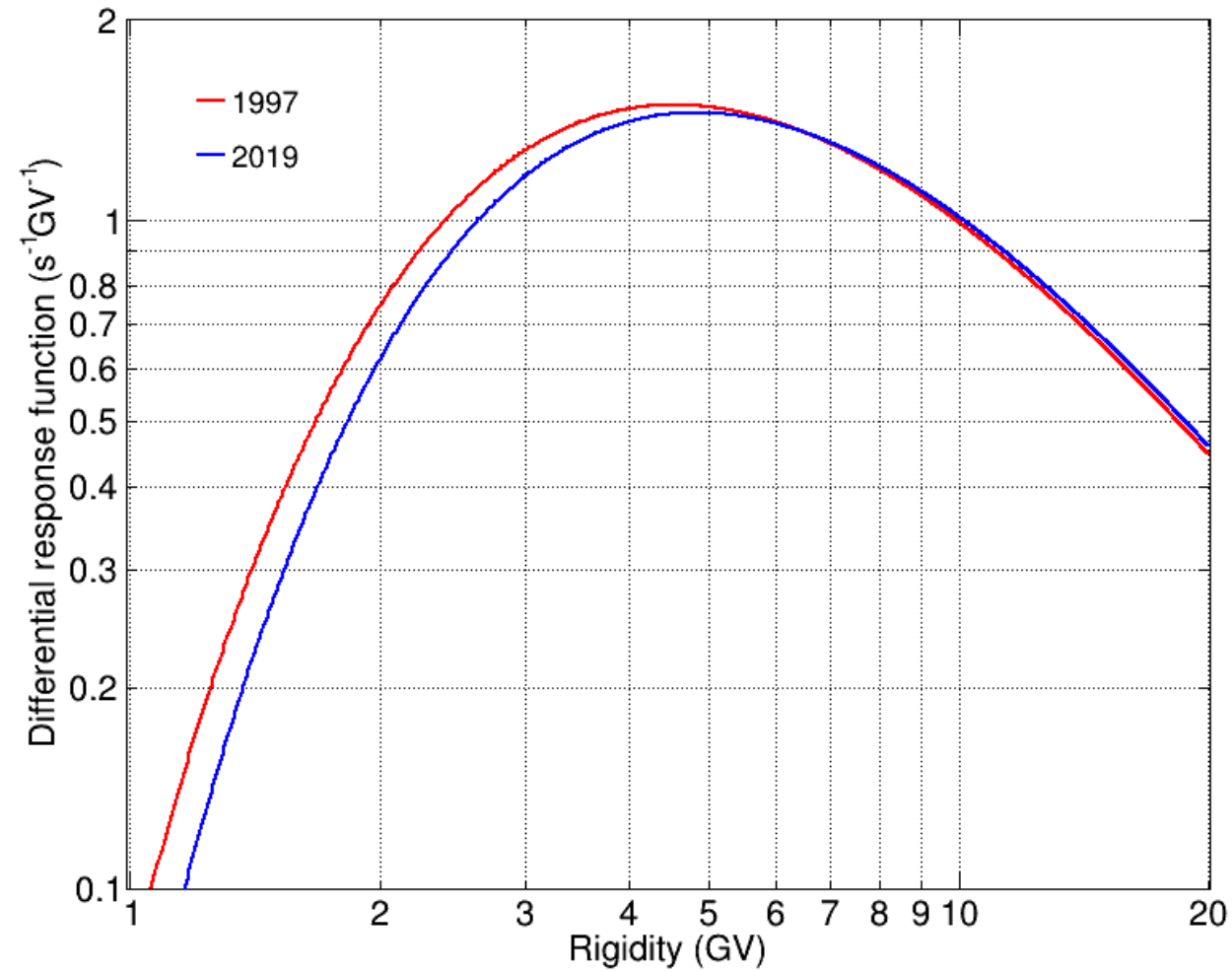
- Used Dorman Parameter from yakum et al., 2021->fit data by group data into rigidity bin and find mean value of each bin

Year	No	alpha	kappa
2018	8.87	6.84	0.807
2019	8.96	8.54	0.881

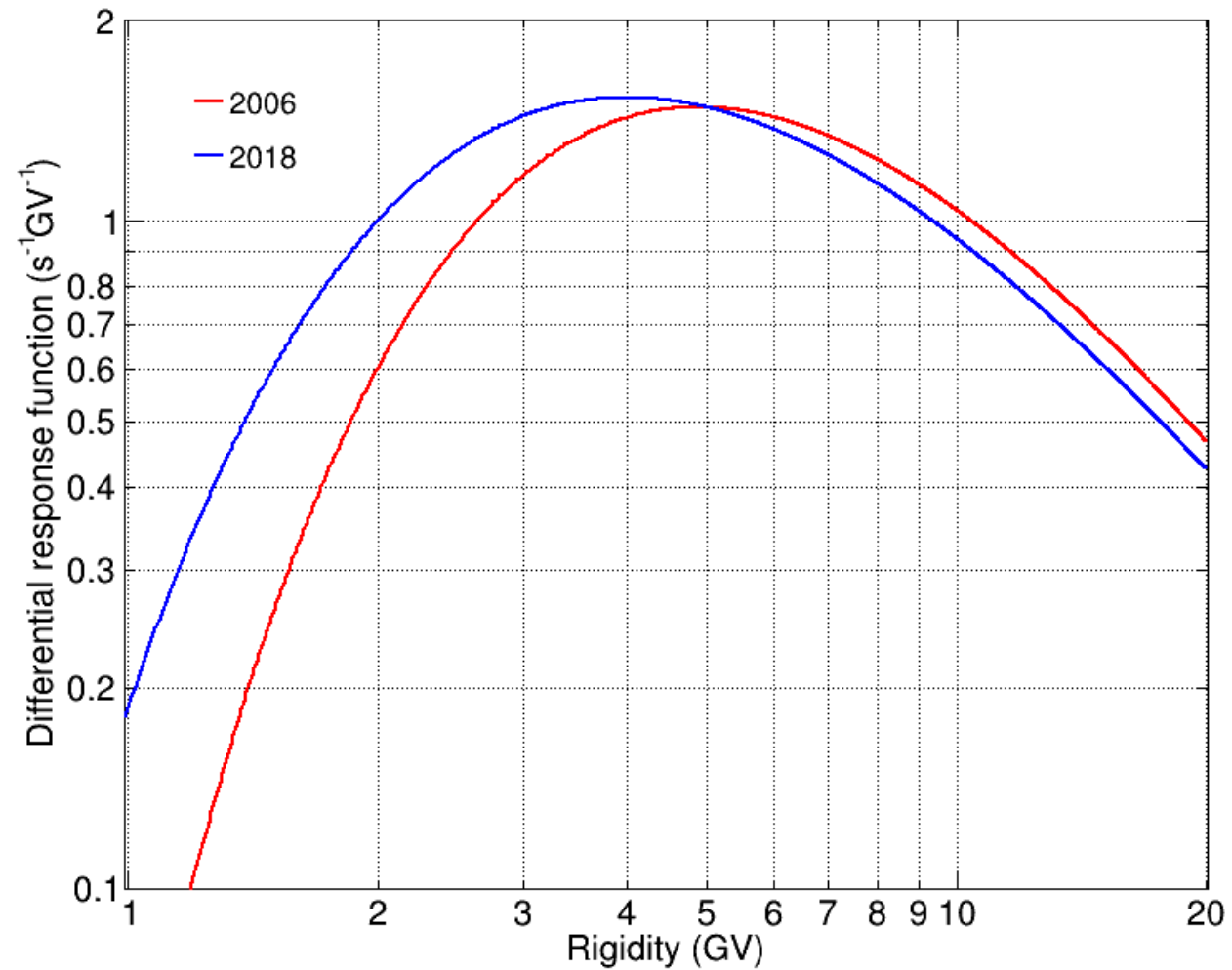




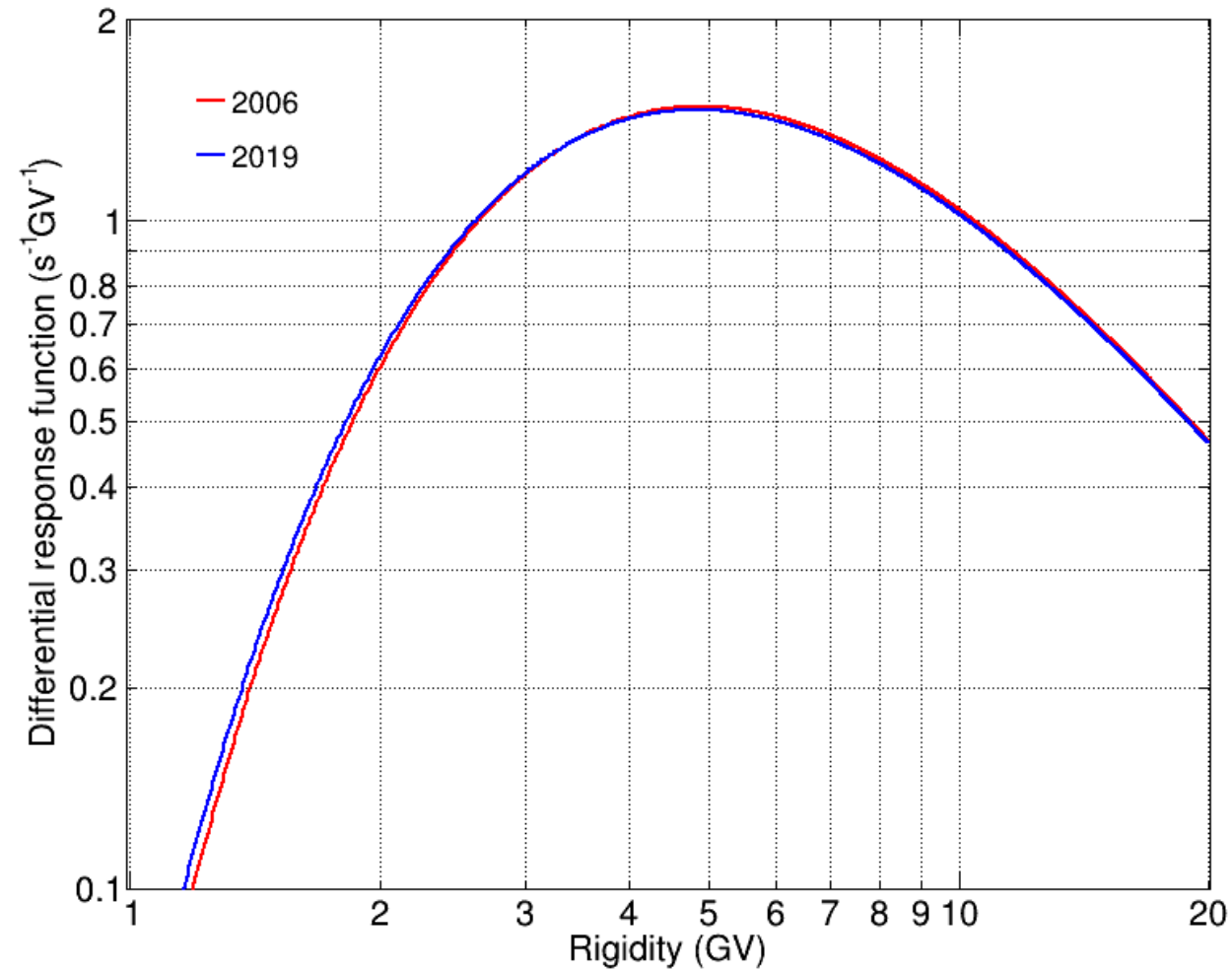
DRF of year 1997 (positive) and 2018 (positive)



DRF of year 1997 (positive) and 2018 (positive)



DRF of year 1997 (positive) and 2018 (positive)



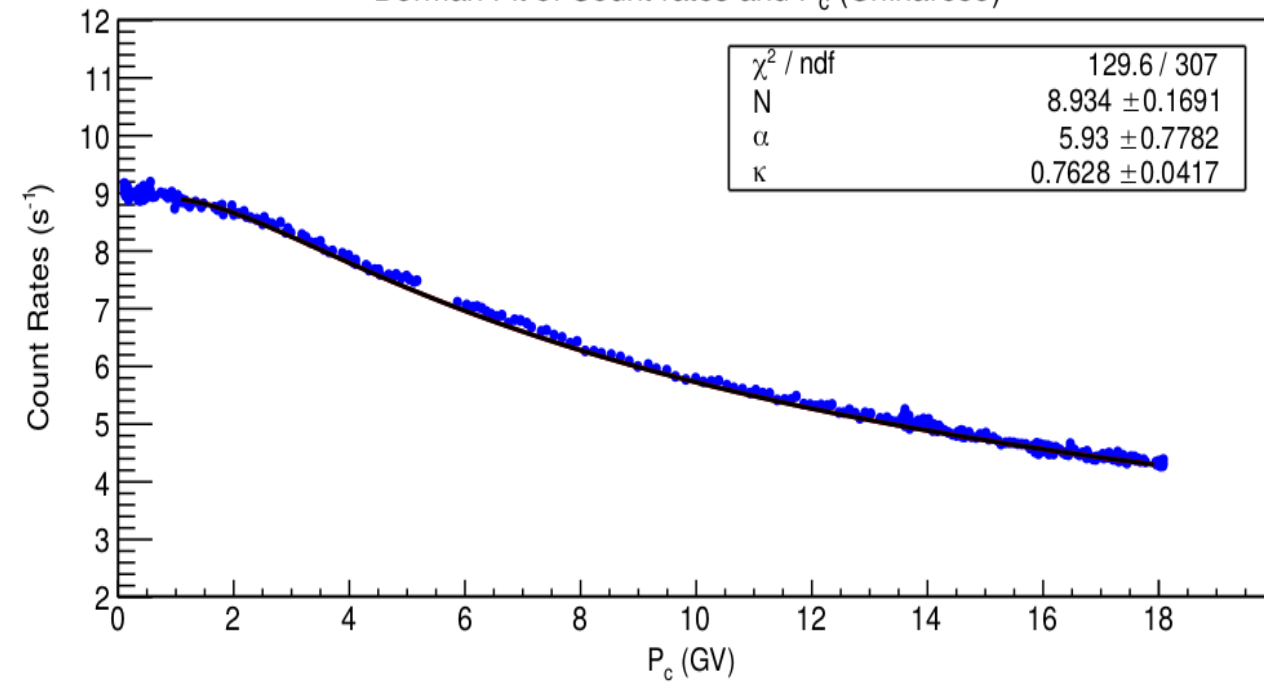
DRF of year 1997 (positive) and 2018 (positive)

Update Dorman Function 2018-2019 (20Dec21)

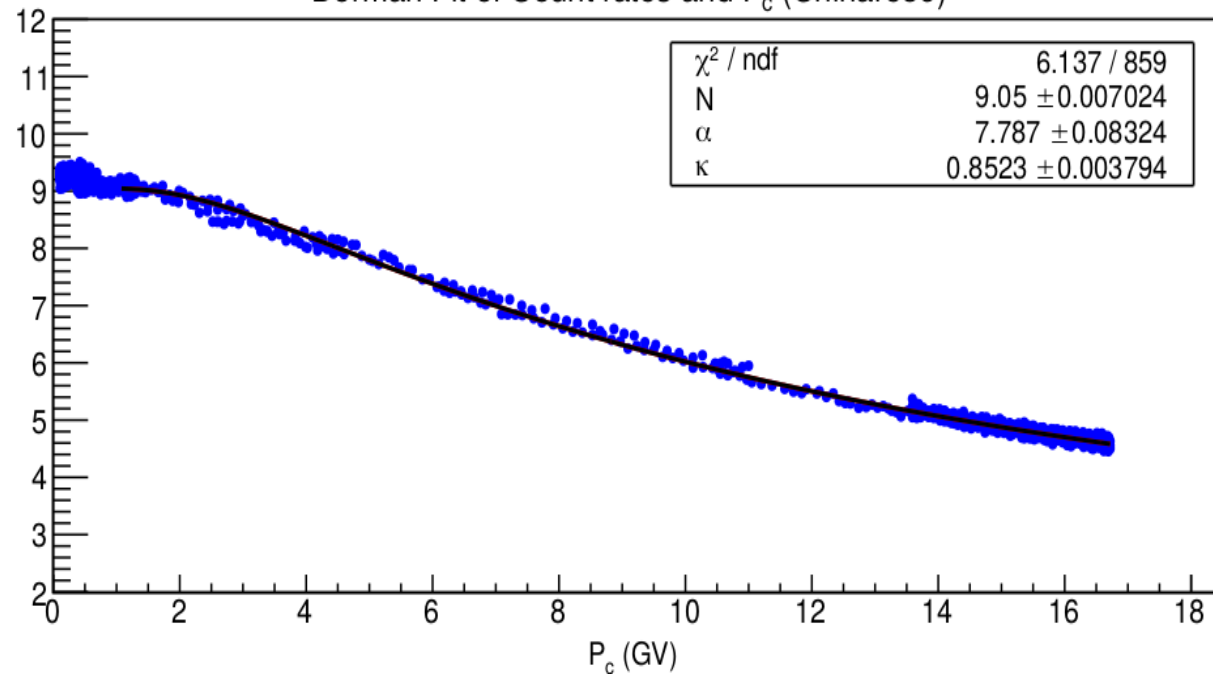
- Used Dorman Parameter from Fern จากการปรับการ fit โดยใช้ข้อมูลทั้งหมดแทนค่าเฉลี่ย cutoff bin แทนค่ะ

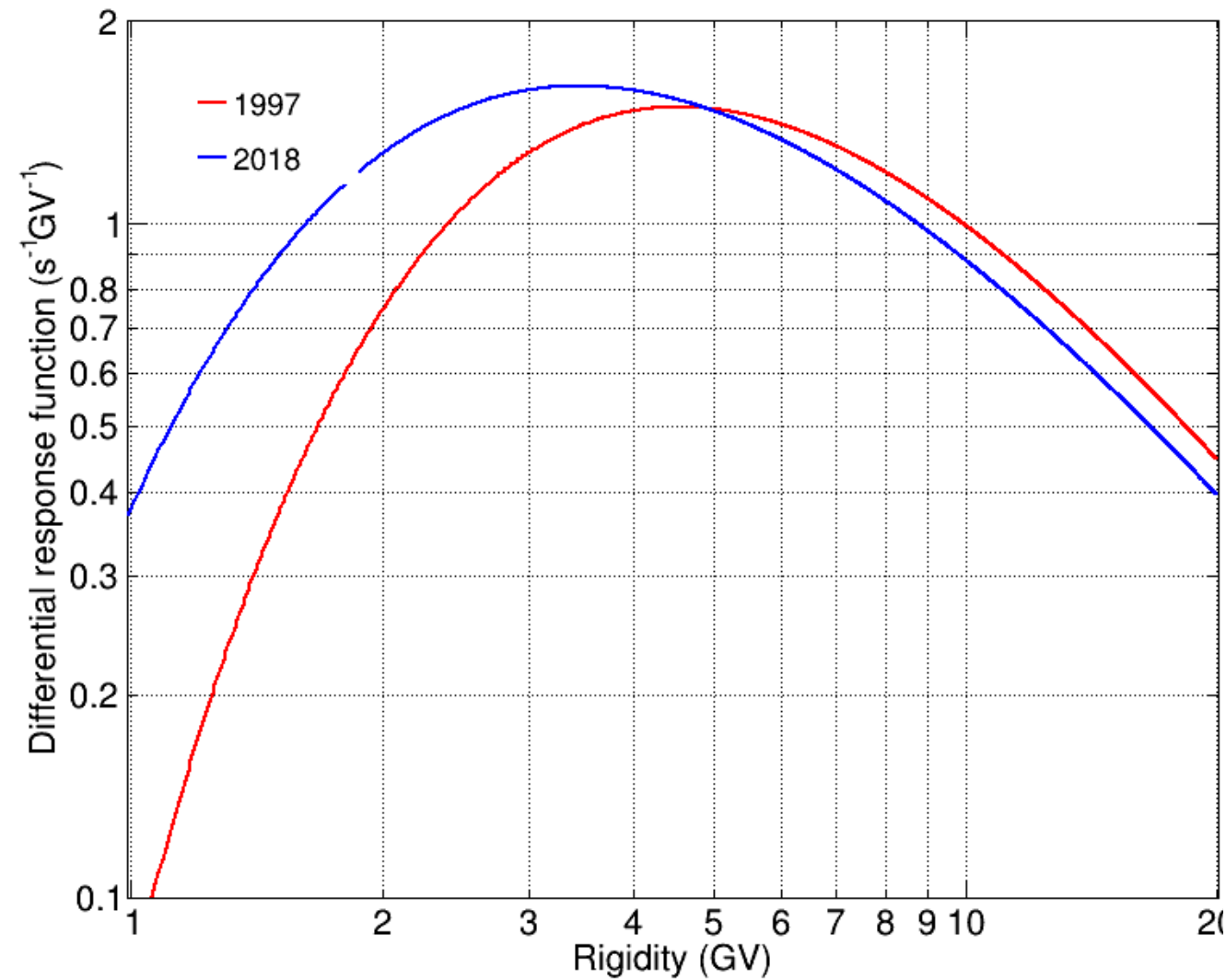
Year	No	alpha	kappa
2018	8.93	5.93	0.763
2019	9.05	7.787	0.852

Dorman Fit of Count rates and P_c (Chinare35)

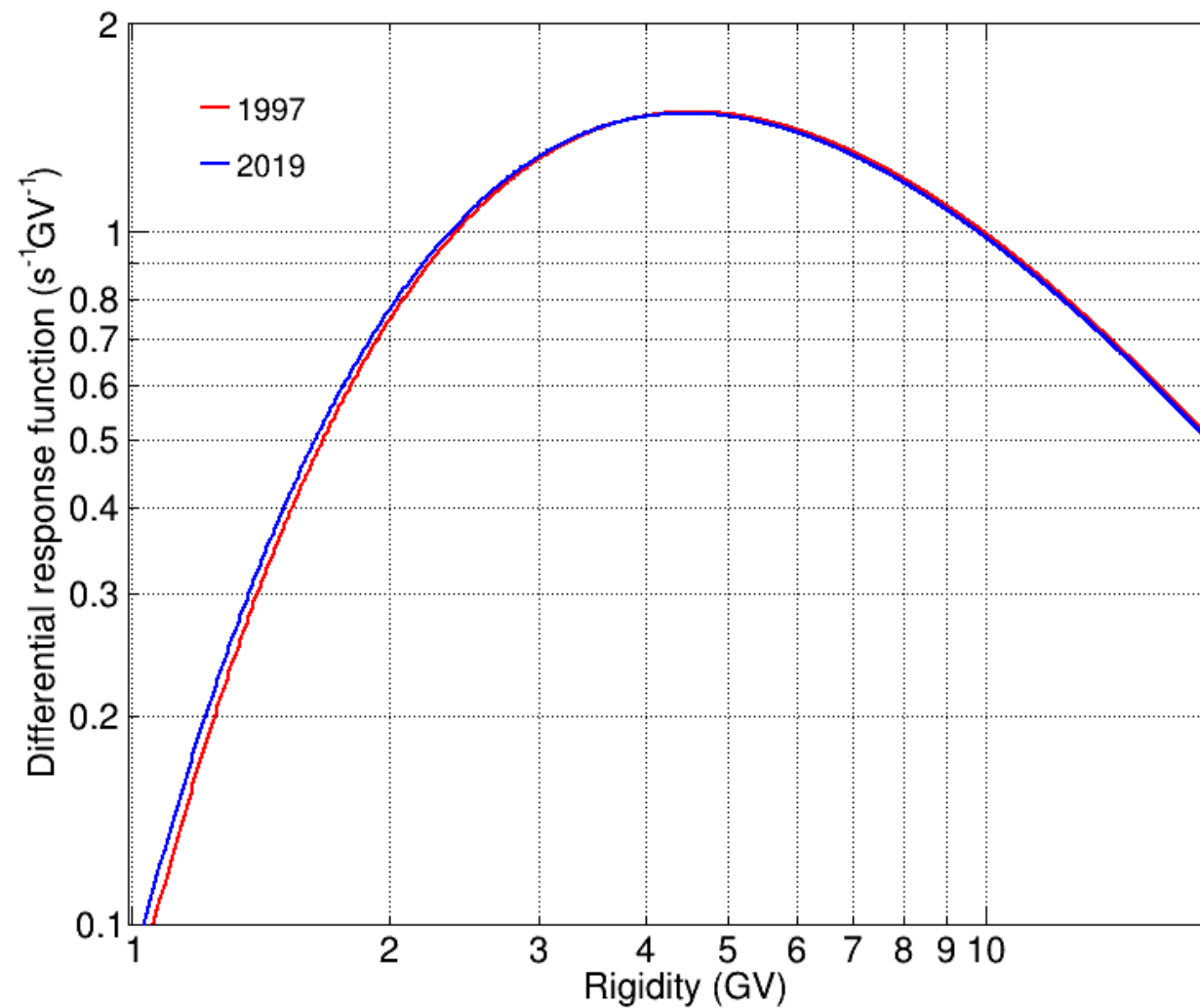


Dorman Fit of Count rates and P_c (Chinare36)

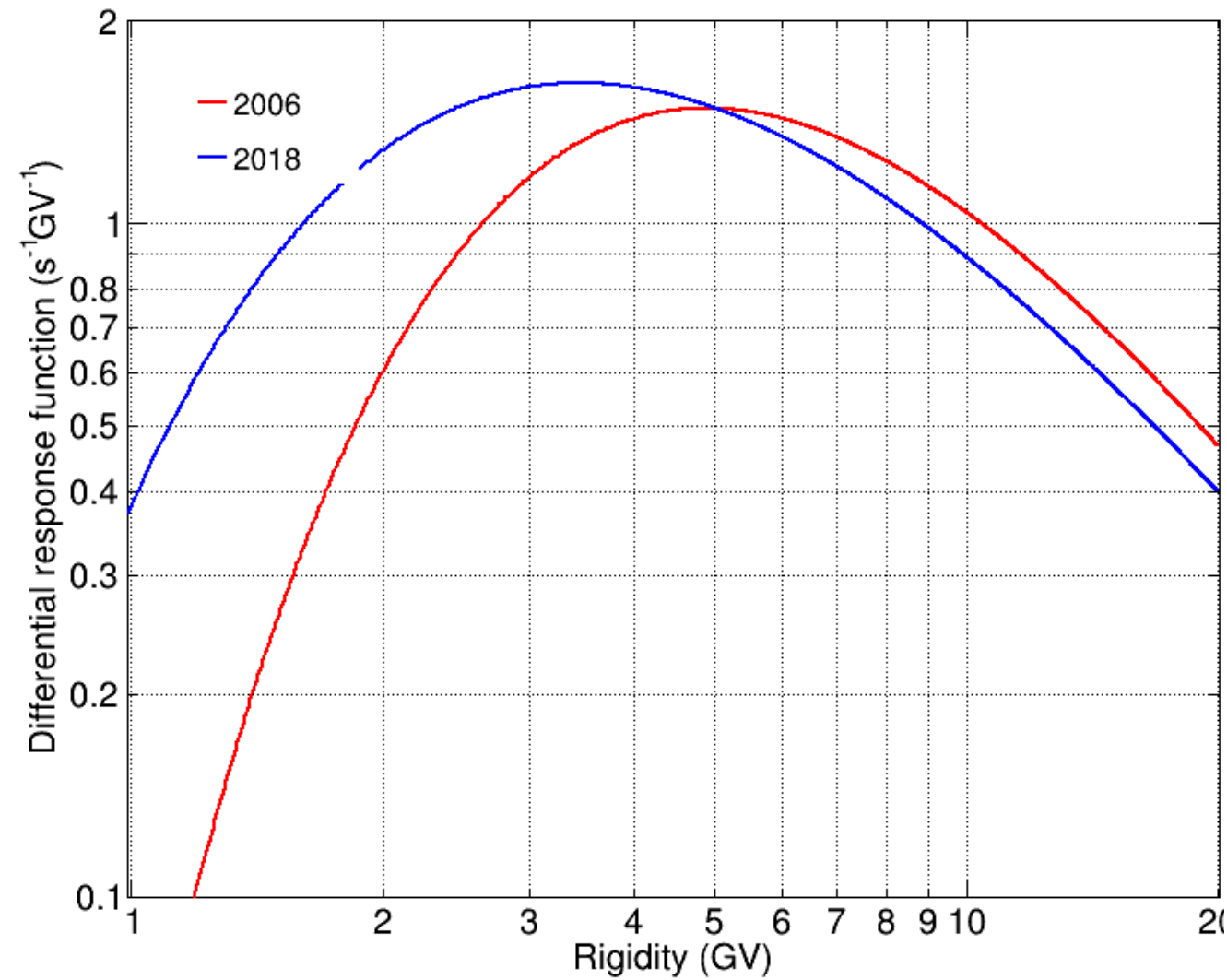




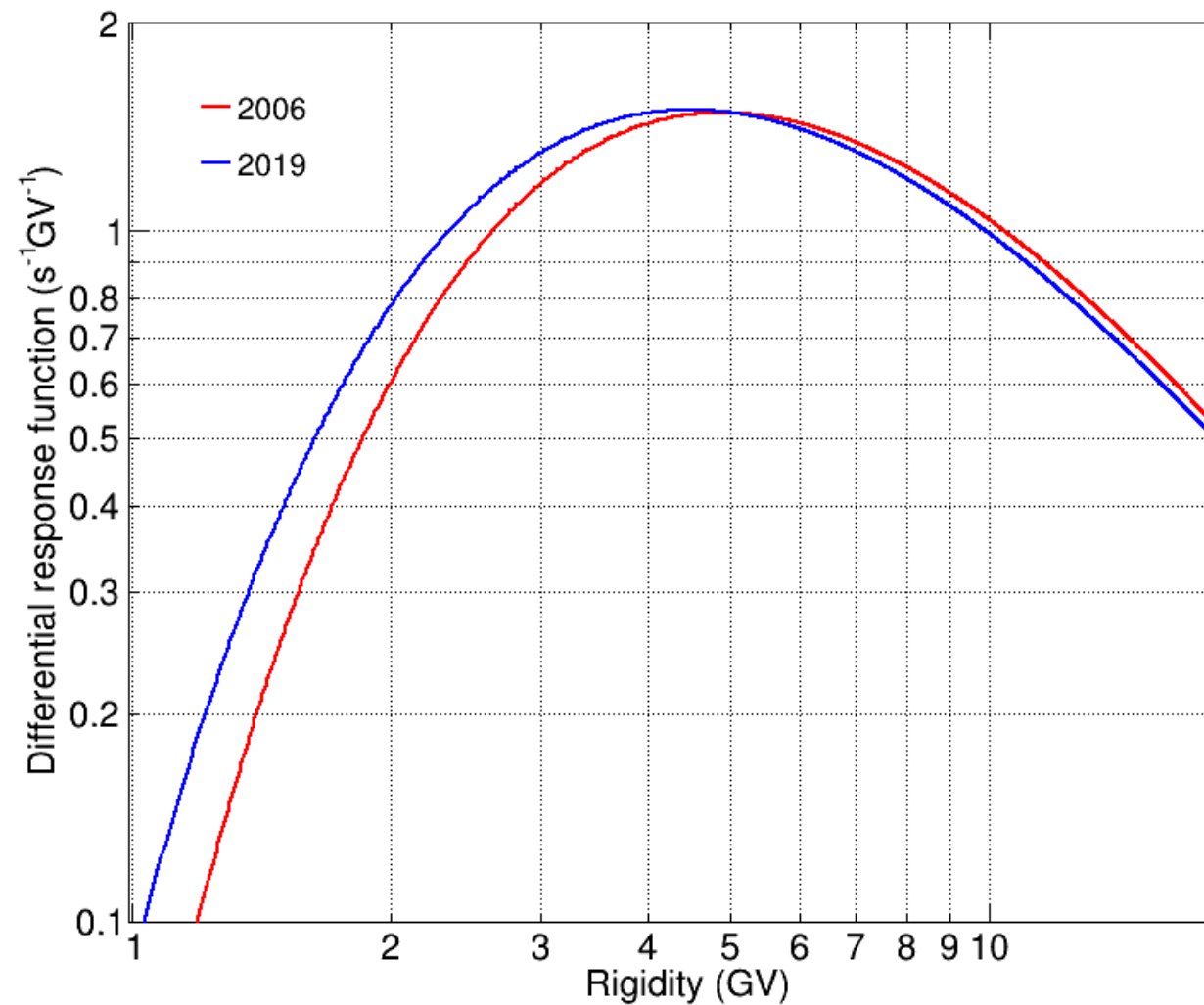
DRF of year 1997 (positive) and 2018 (positive)



DRF of year 1997 (positive) and 2018 (positive)

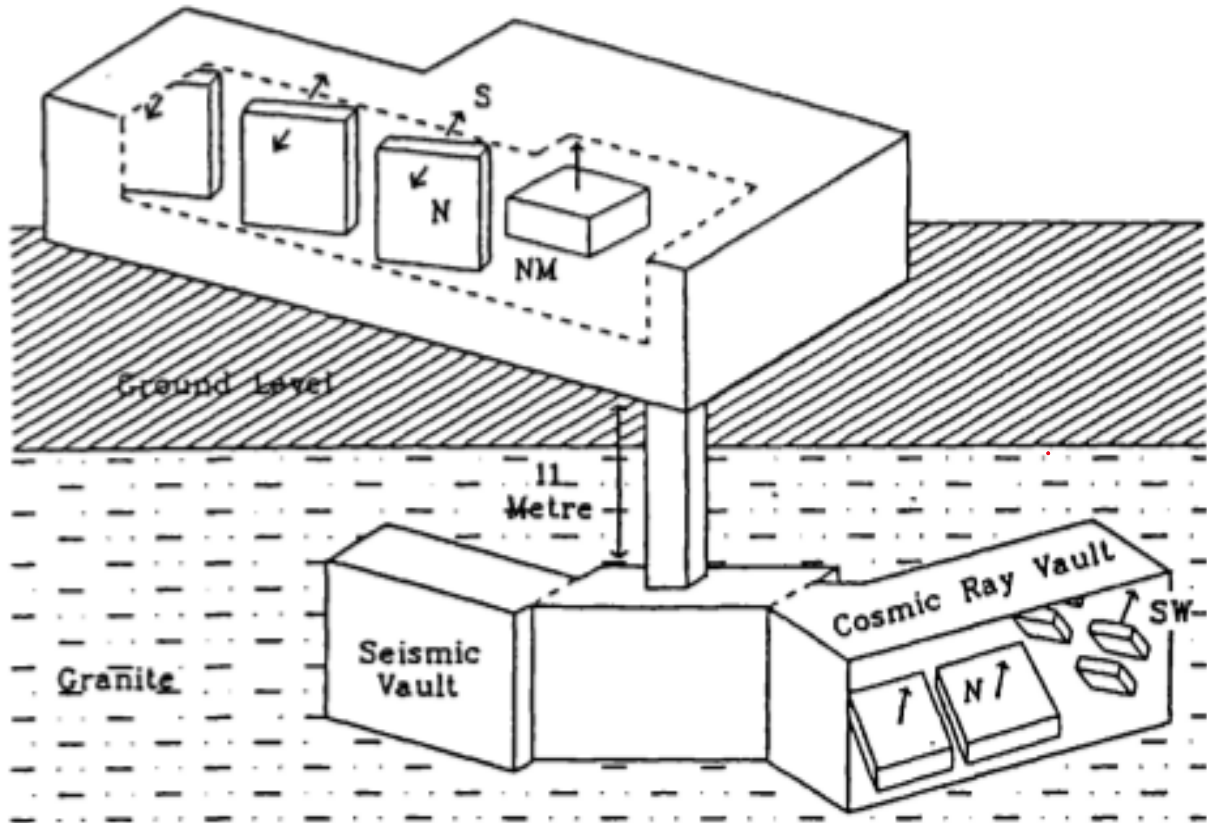


DRF of year 2006 (negative) and 2018 (positive)



DRF of year 2006 (negative) and 2019 (positive)

MAWSON MUON TELESCOPE



Geometry of Mawson station



Summary of muon telescope parameters at the Mawson Automated Cosmic Ray Observatory.

	SURFACE		UNDERGROUND	
	NORTH	SOUTH	NORTH	SOUTH WEST
Cutoff Rigidity	13 GV	13 GV	13 GV	13 GV
Effective Median Rigidity	35-200 GV	190 GV	35-200 GV	180 GV
Azimuth	North	South	330°	215°
Zenith	34° -84°	34° -84°	24°	40°
Absorber	.13m (steel)	.13m (steel)	48 m.w.e. (granite)	53 m.w.e. (granite)

THE DATA OF MUON TELESCOPE

```
xml version="1.0"?>
- CDU Data File -->
daily>
  <year>2013</year>
  <day>100</day>
  <station>
    <name>Mawson</name>
    <latitude>67 deg 36 min South</latitude>
    <longitude>62 deg 52 min East</longitude>
  </station>
  <telescope>
    <name>p1</name>
    <eht units="Volts">2275.0</eht>
    <total_tubes>48</total_tubes>
    <tubes_per_wall>24</tubes_per_wall>
  </telescope>
  <comments>Telescope P1 is a surface muon telescope located at Mawson station, Antarctica.</comments>
  <record endtime="00:01:00" period="60">
    <coincidentals>13,12,22,29,28,51,67,78,102,108,152,176,188,229,244,239,215,208,146,127,83,56,38,36,40,62,82,103,16
    <accidentals>1,0,3,3,3,3,5,2,3,3,10,6,7,12,9,6,15,4,11,11,9,8,11,11,8,9,15,10,4,8,8,8,10,9,6,6,8,4,4,5,4,4,2,2,4,0,0</accide
  </record>
  <record endtime="00:02:00" period="60">
    <coincidentals>15,12,14,25,34,52,56,65,102,122,152,169,20
    <accidentals>2,1,4,3,3,4,8,2,5,6,0,11,2,7,14,6,7,7,10,12,13,
  </record>
```

← Date and time

location


Telescope detail

Recorded data

Accidental vs Coincidental rate

Accidental rate = independent particles pass through difference trays

Coincidental rate = a single particle pass through both trays

 the accidental rate can be removed to give the true coincidence rate.

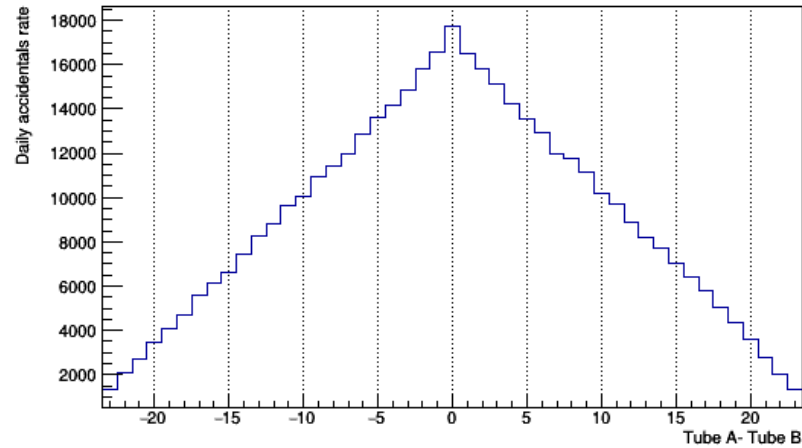
When $\tau \ll 1/C$
and for $\tau_2 = 2\tau_1$
solving for C gives
and

$$\begin{aligned}R(\tau) &= C + A(\tau) \\A(\tau_2) &= 2A(\tau_1) \\C &= 2R(\tau_1) - R(\tau_2) \\A(\tau_1) &= R(\tau_2) - R(\tau_1)\end{aligned}$$

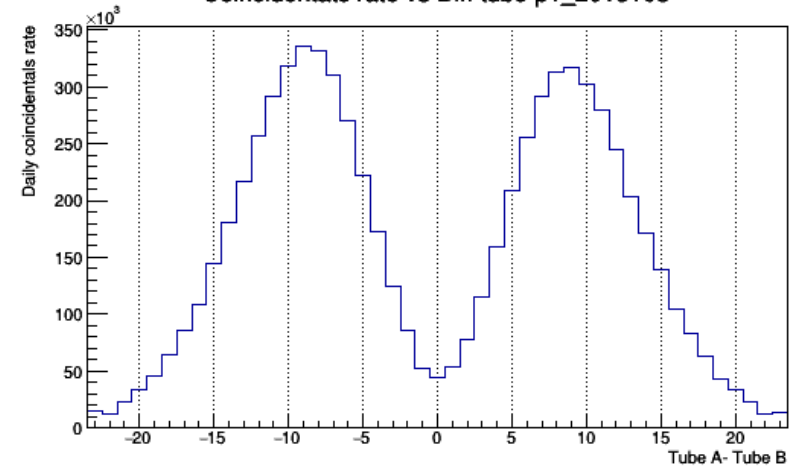
The coincidence rate for the new telescope is 180000 particles/hour (i.e. the average time between particles is 20 ms)

Surface Muon Telescopes

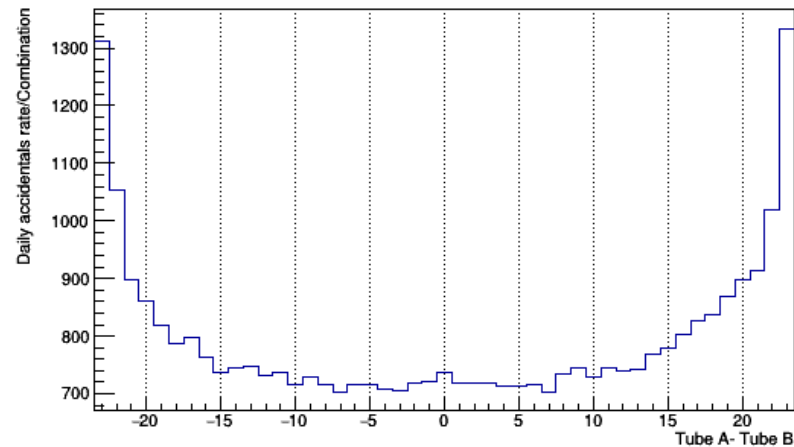
Accidentals rate vs Diff tube p1



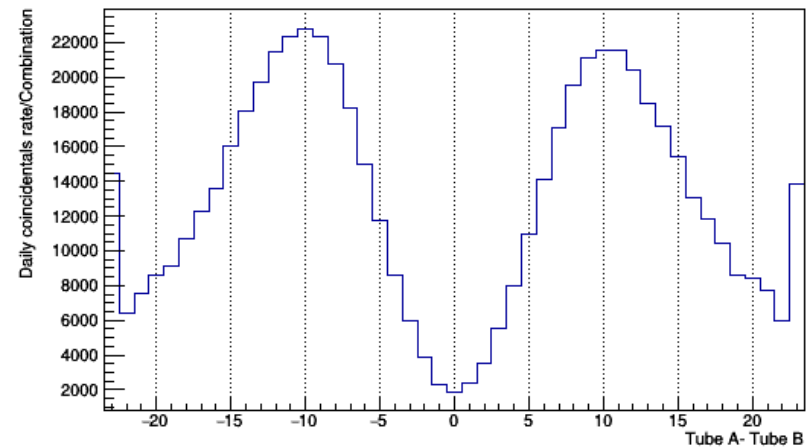
Coincidentats rate vs Diff tube p1_2013103



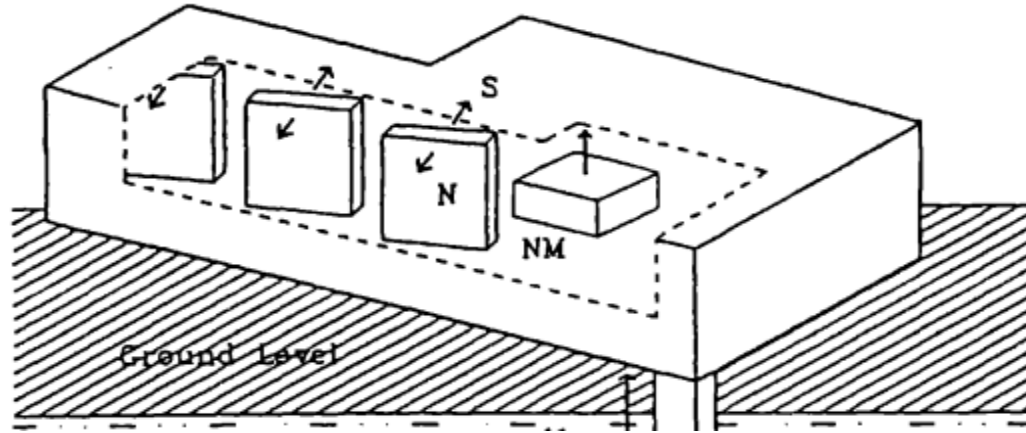
Accidentals rate/Combination vs Diff tube p1_2013103



Coincidentats rate/Combination vs Diff tube p1_2013103



ground Level



- P1, 2 & 3 have effective mean Rigidity 35-200 GV both north and south and have 0.13m steel absorber between the counter walls.

P1, 2 & 3 North view equatorial to mid southern latitudes. Effective mean Rigidity 35-200 GV.

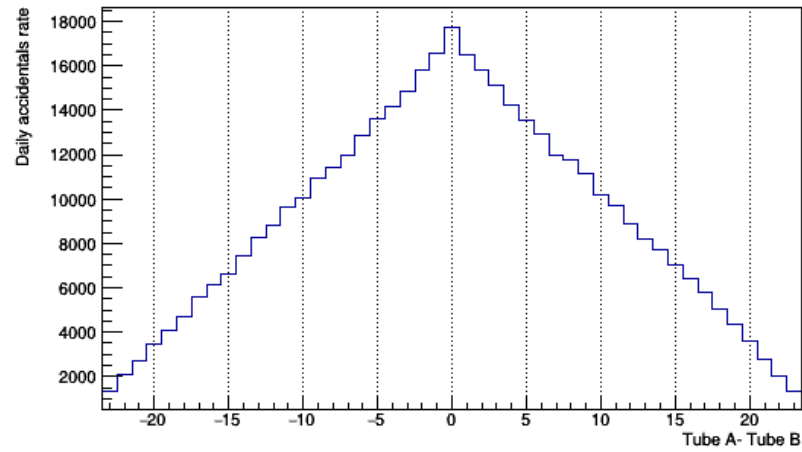
P1, 2 & 3 South view across the south pole into the opposite temporal hemisphere but have maximum geomagnetic deflection due to viewing across the field and so effectively spread spectral phenomena out in time. Effective mean Rigidity 35-200 GV.

Manson Muon zenith angle

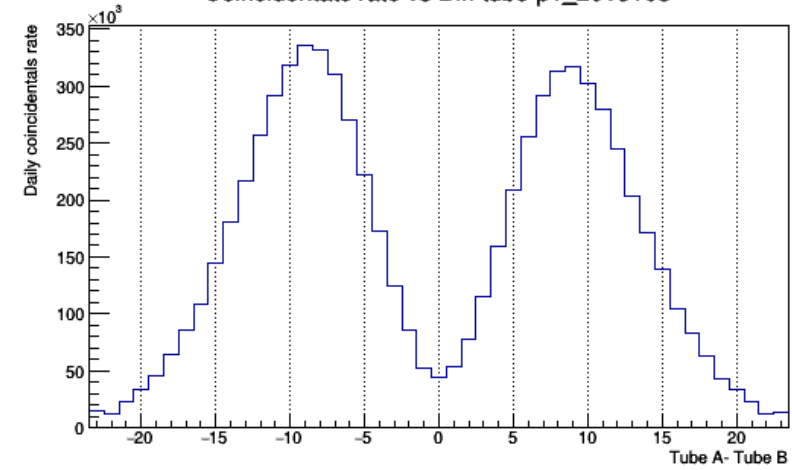
P1, 2 & 3

P1

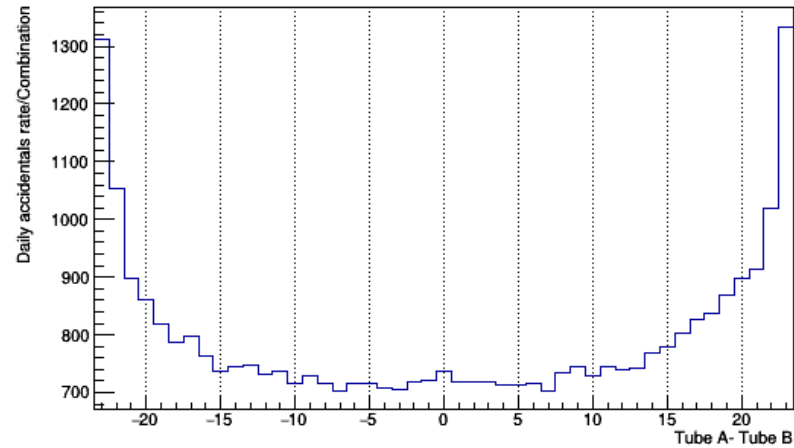
Accidentats rate vs Diff tube p1



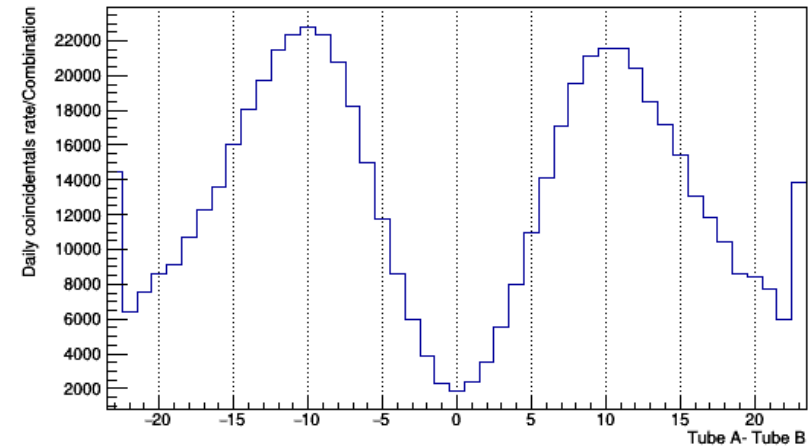
Coincidentats rate vs Diff tube p1_2013103



Accidentats rate/Combination vs Diff tube p1_2013103

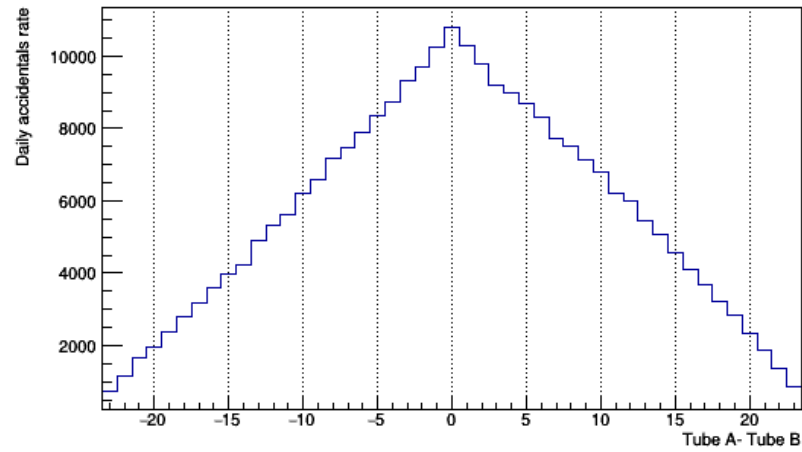


Coincidentats rate/Combination vs Diff tube p1_2013103

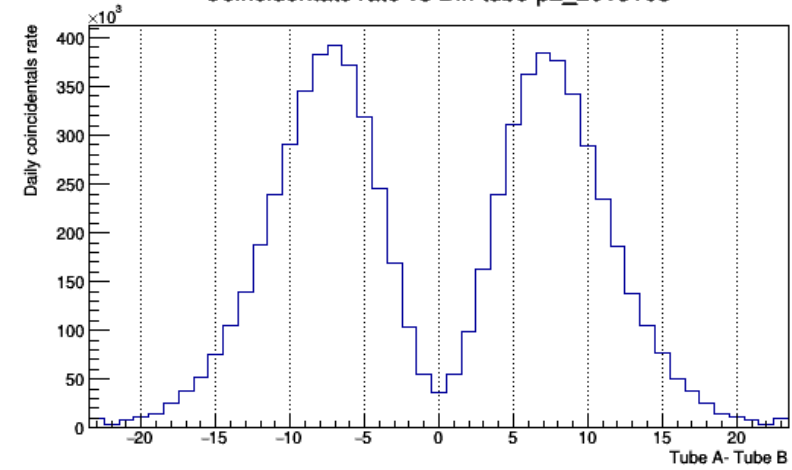


P2

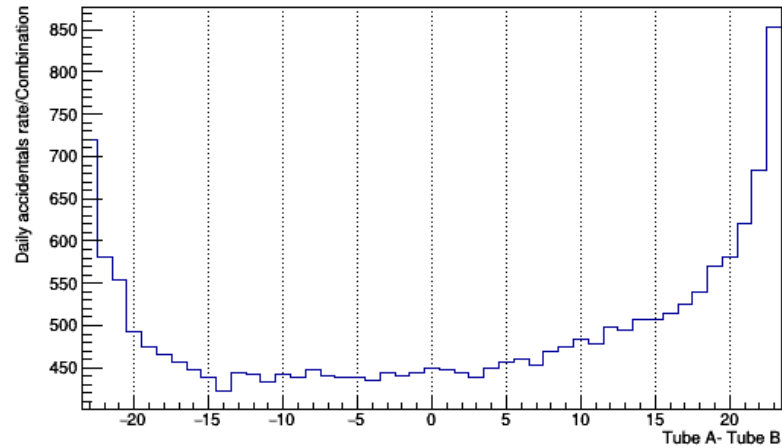
Accidentats rate vs Diff tube p2



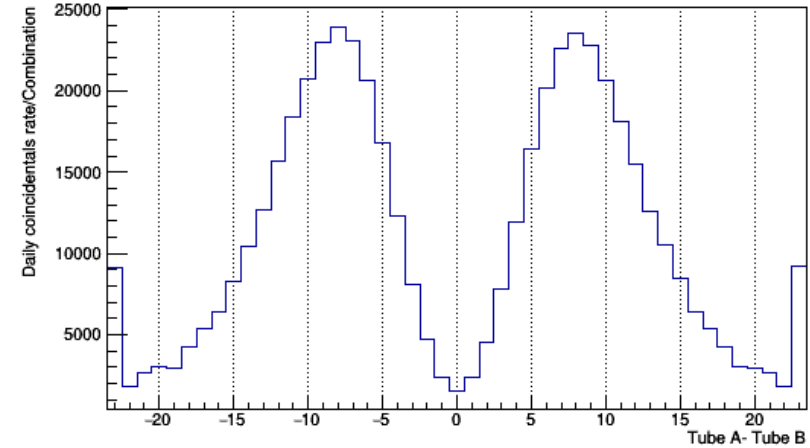
Coincidentats rate vs Diff tube p2_2013103



Accidentats rate/Combination vs Diff tube p2_2013103

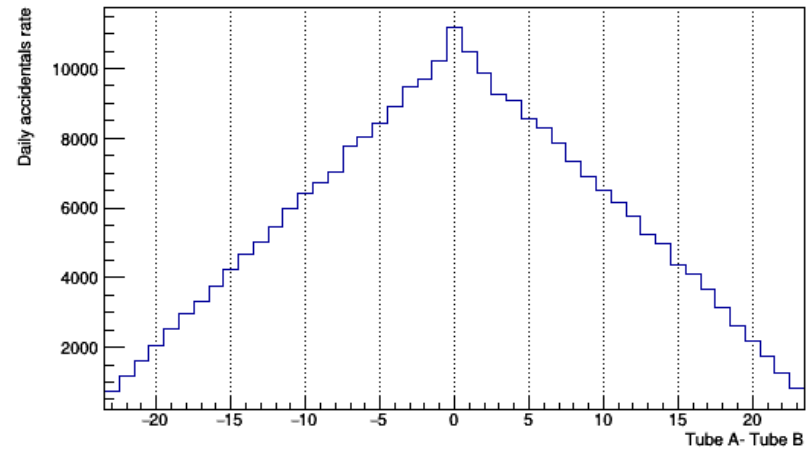


Coincidentats rate/Combination vs Diff tube p2_2013103

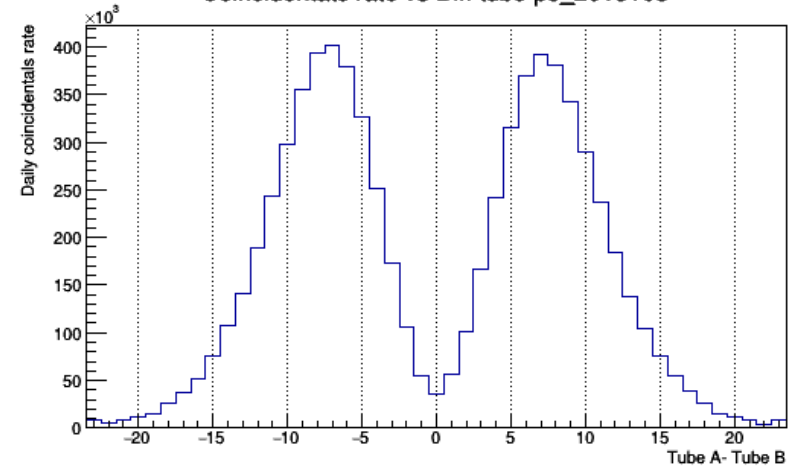


P3

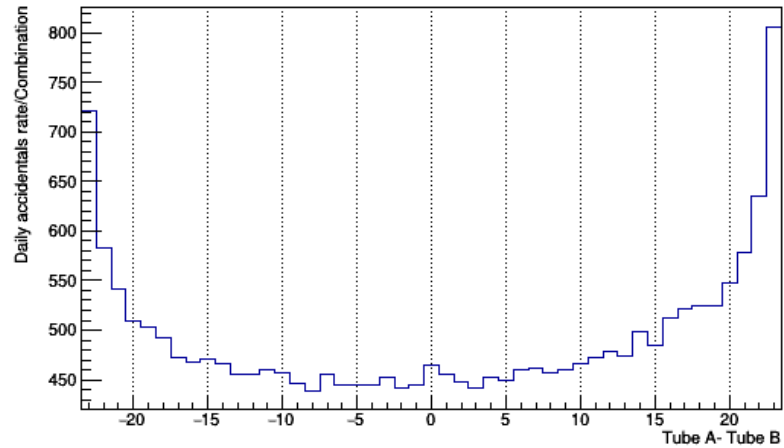
Accidentals rate vs Diff tube p3



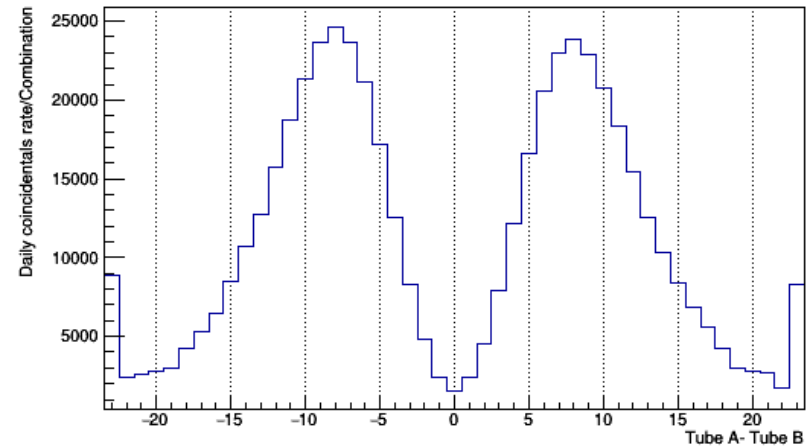
Coincidentats rate vs Diff tube p3_2013103



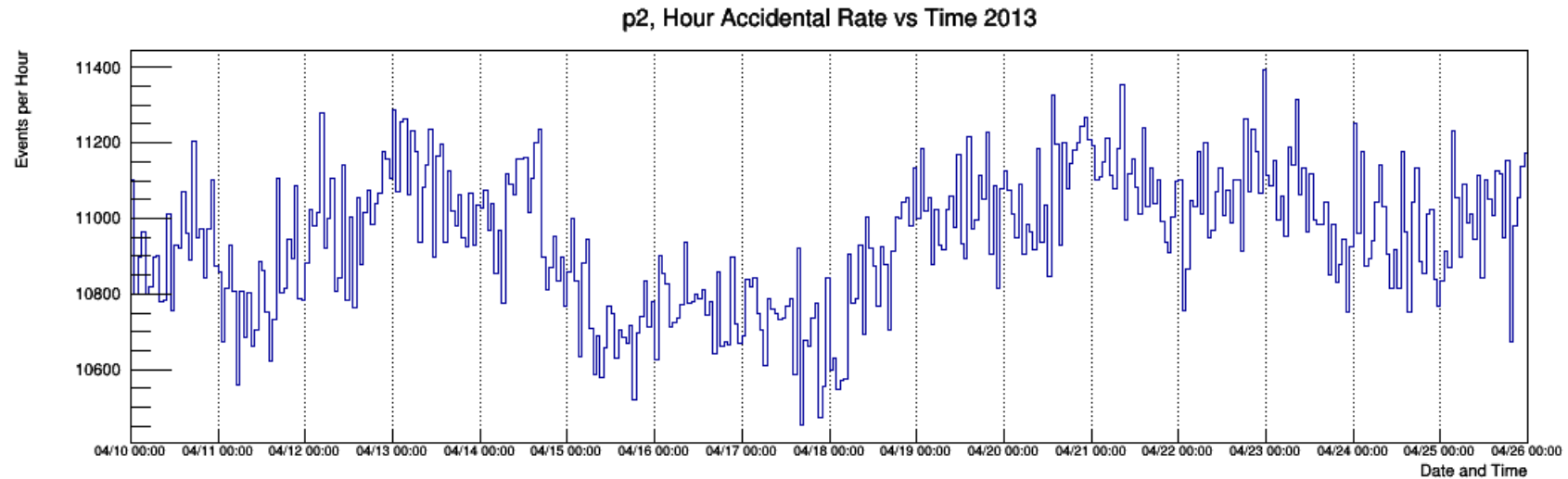
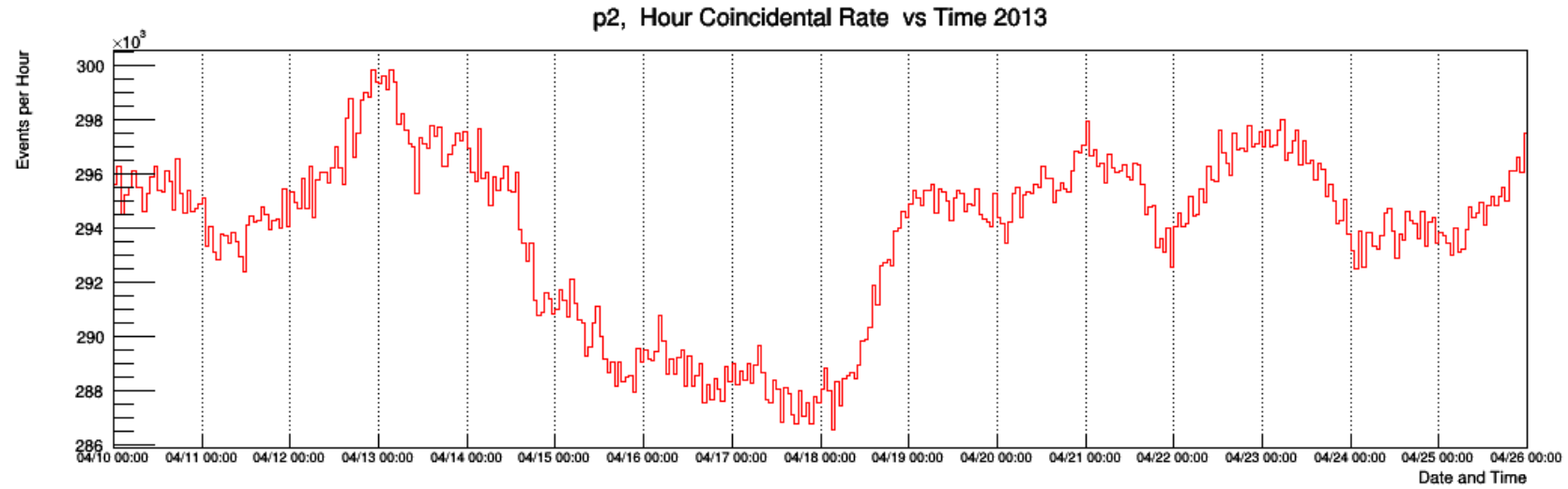
Accidentats rate/Combination vs Diff tube p3_2013103



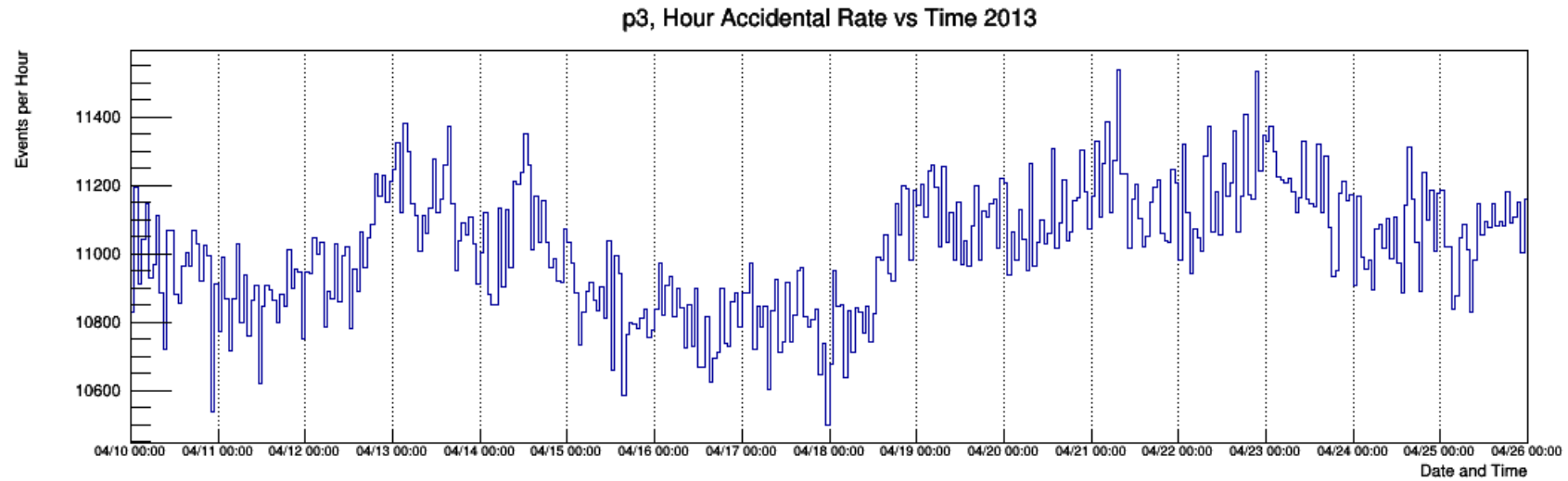
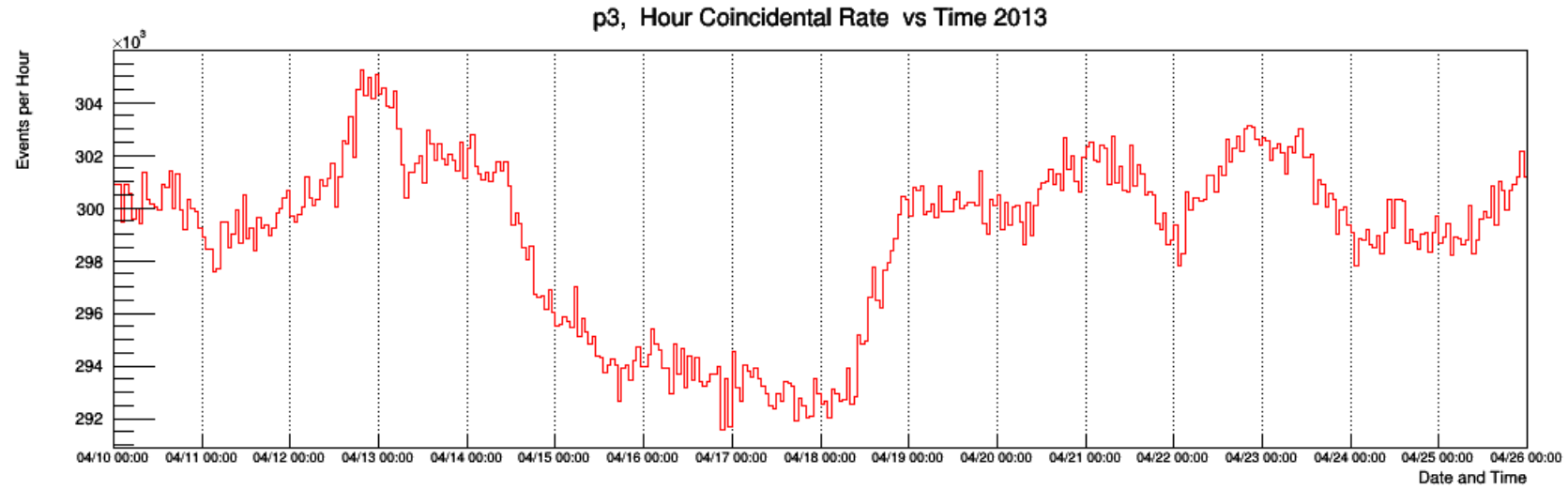
Coincidentats rate/Combination vs Diff tube p3_2013103



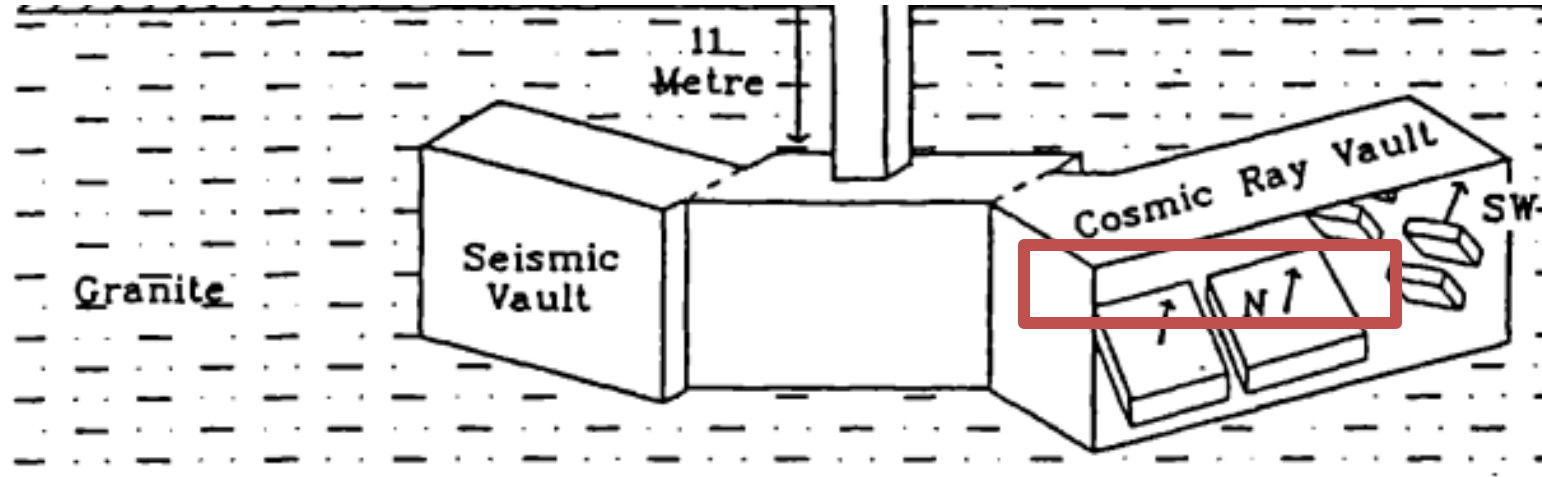
Hour data P2



Hour data P3



Underground Level



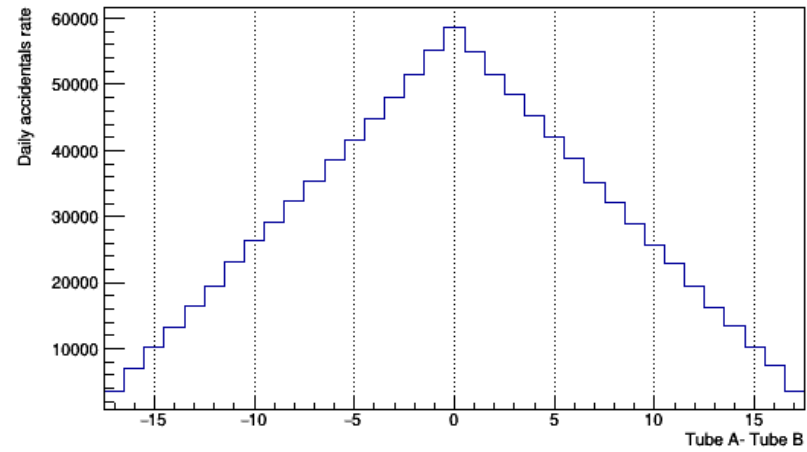
- P6 & 7 view along the local geomagnetic field and thus have minimal geomagnetic deflection and view mid southern latitudes very close to the Mawson NM view. Effective mean Rigidity 180 GV resulting from 48 mwe granite absorber along the central viewing direction.

Manson Muon zenith angle

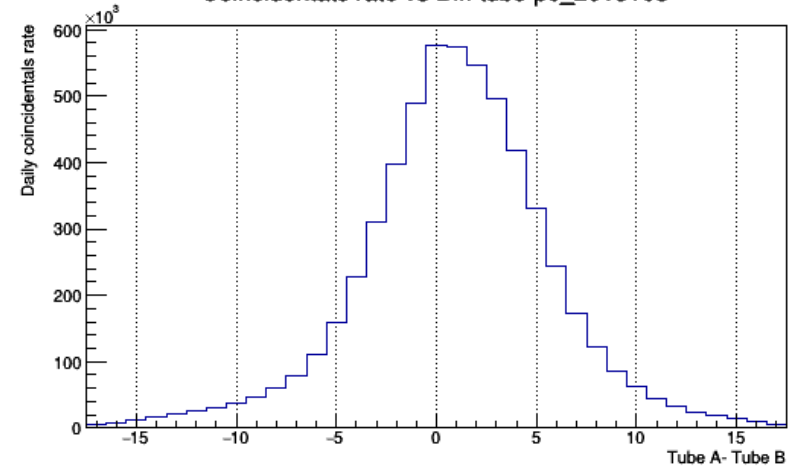
P6 & 7

P6

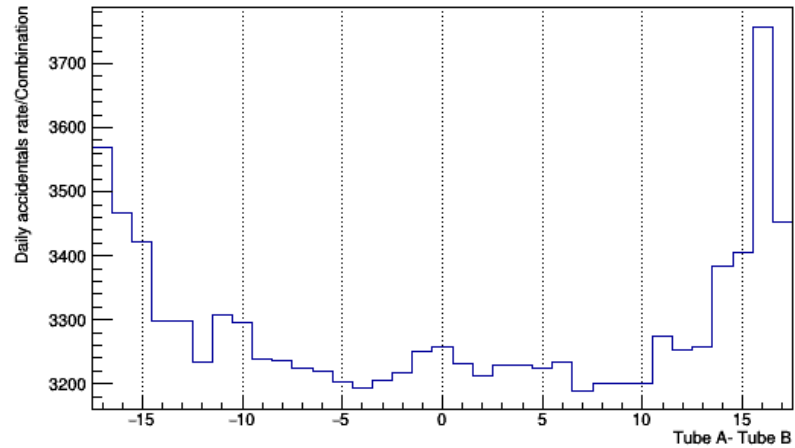
Accidentals rate vs Diff tube p6



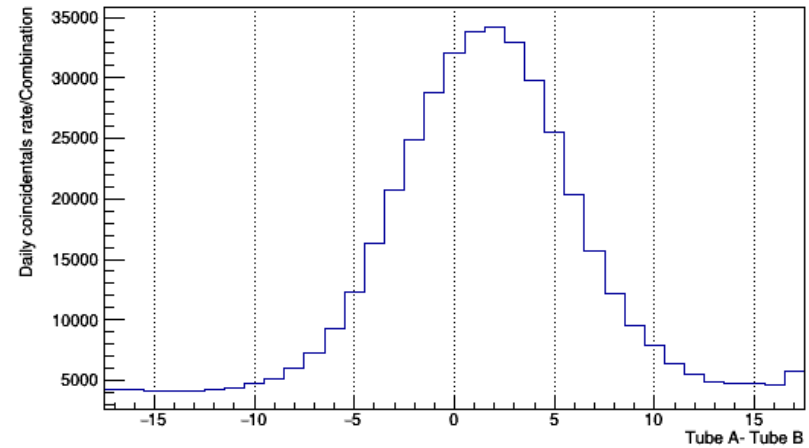
Coincidentats rate vs Diff tube p6_2013103



Accidentals rate/Combination vs Diff tube p6_2013103

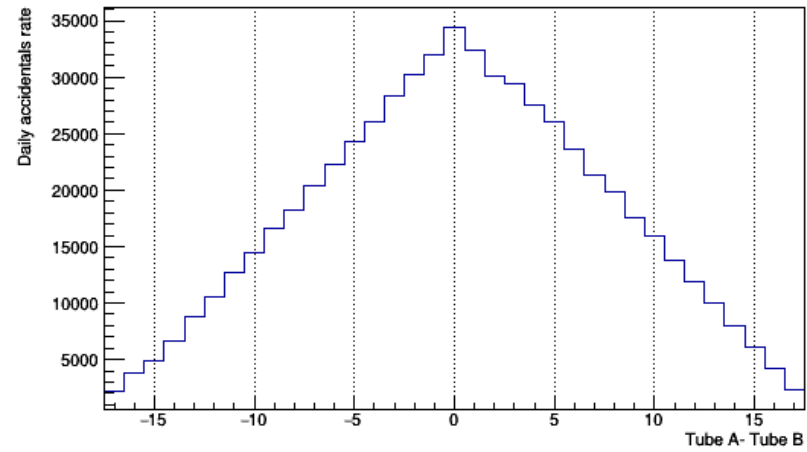


Coincidentats rate/Combination vs Diff tube p6_2013103

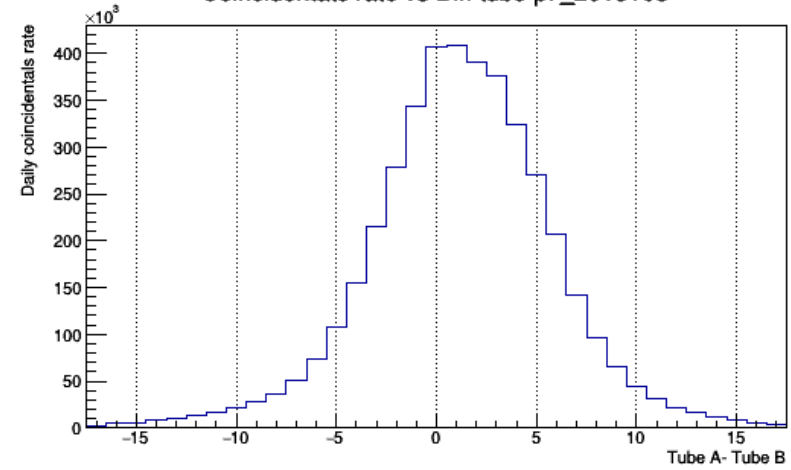


P7

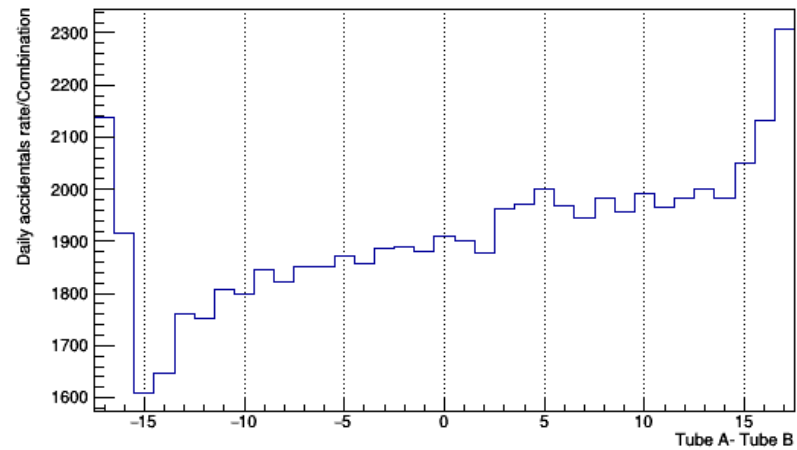
Accidentals rate vs Diff tube p7



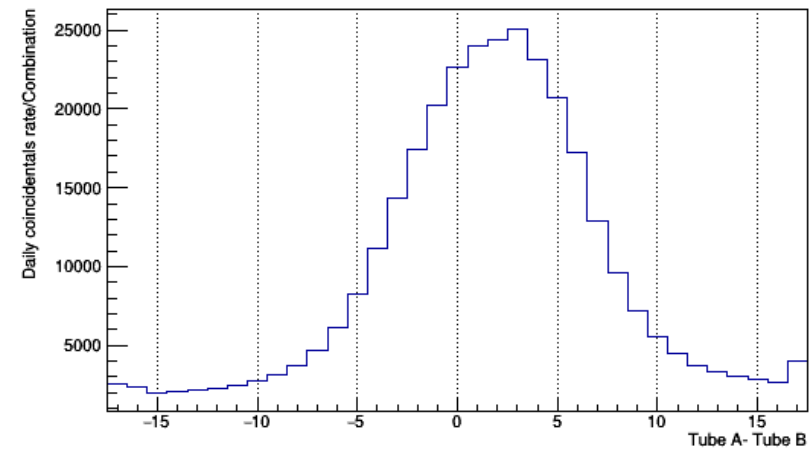
Coincidentats rate vs Diff tube p7_2013103



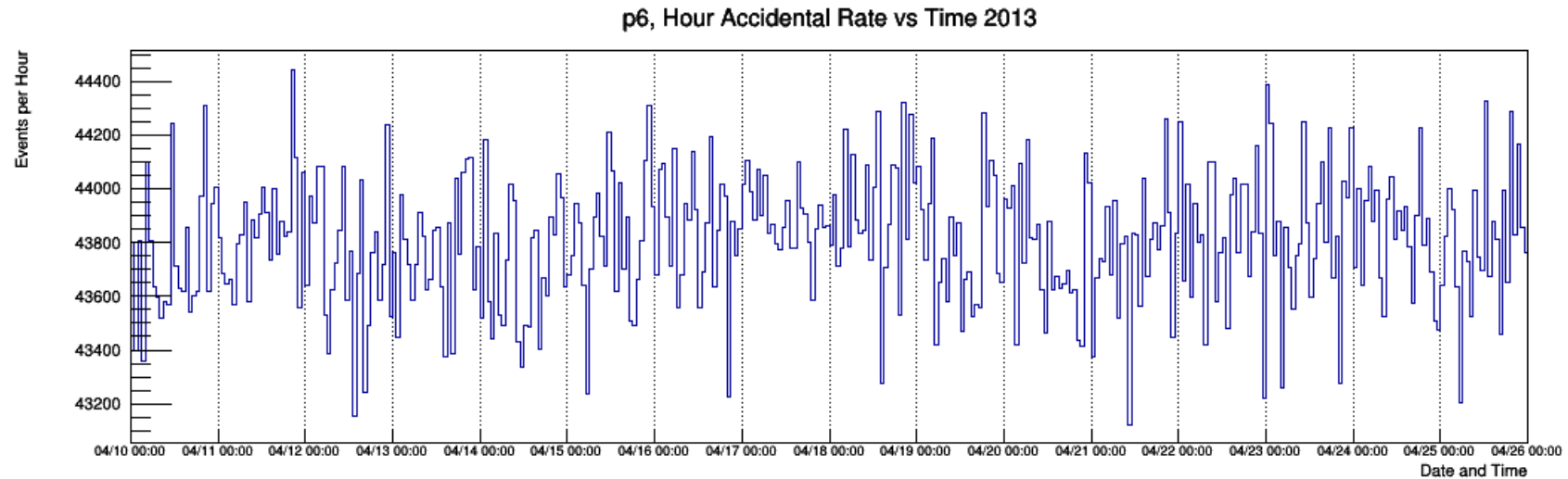
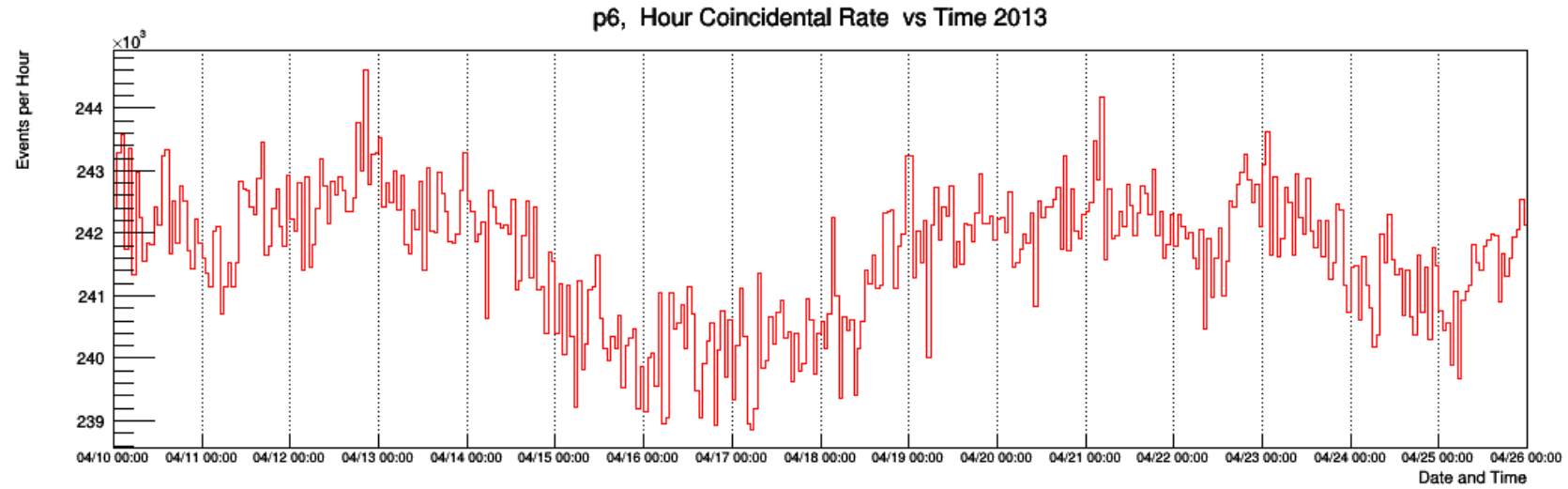
Accidentats rate/Combination vs Diff tube p7_2013103



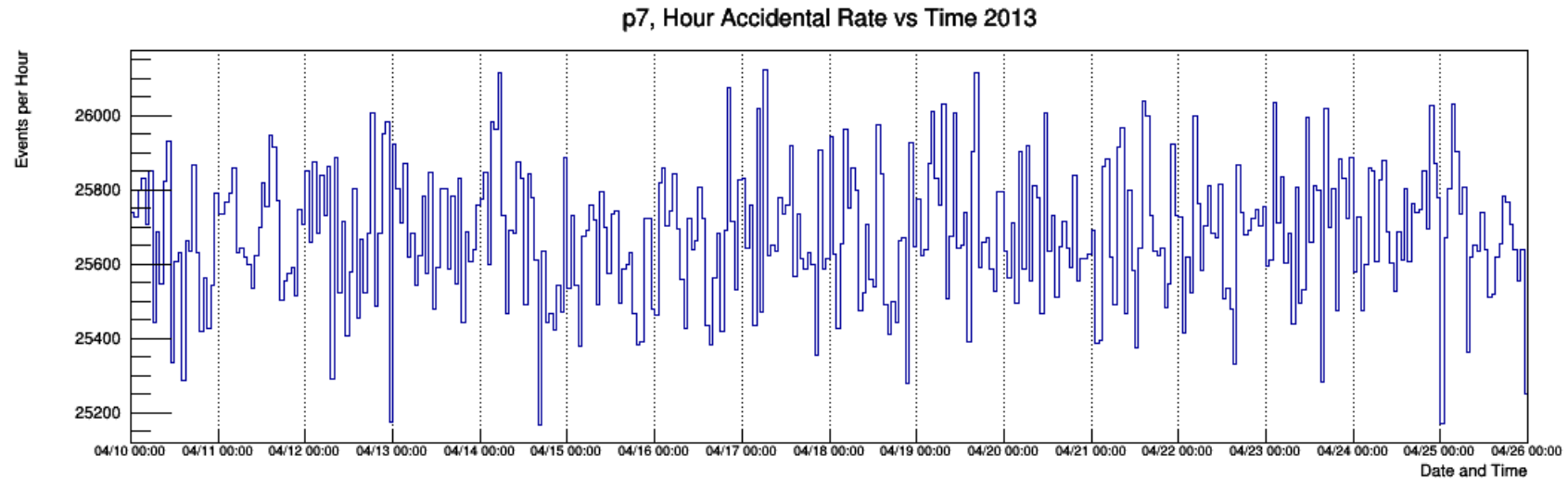
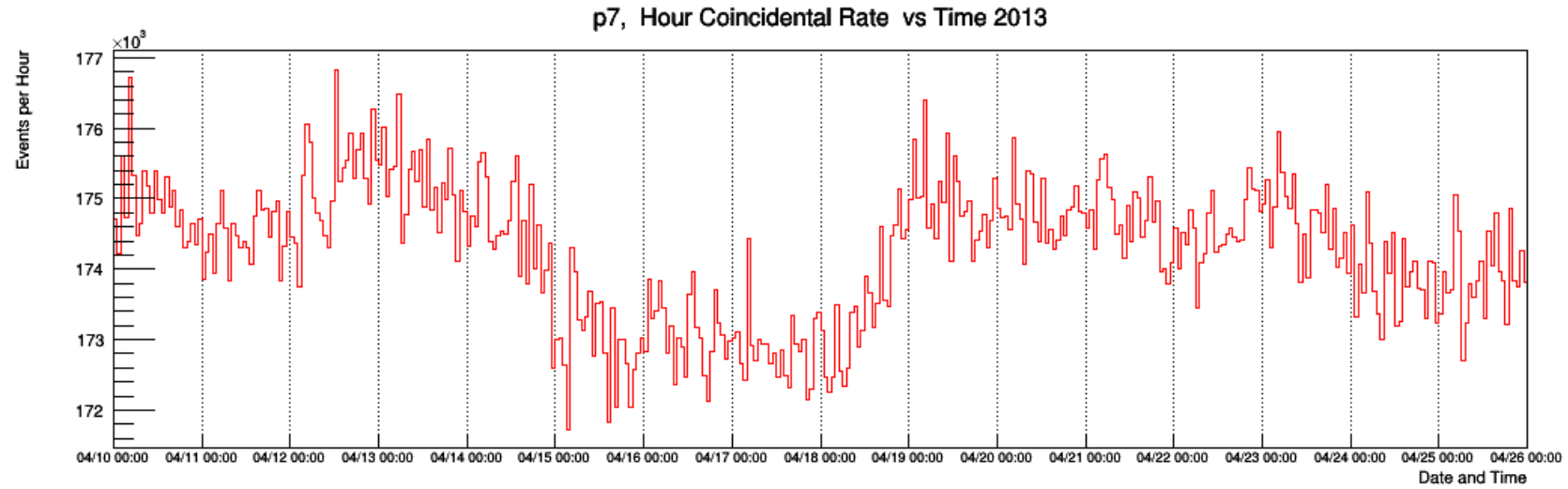
Coincidentats rate/Combination vs Diff tube p7_2013103



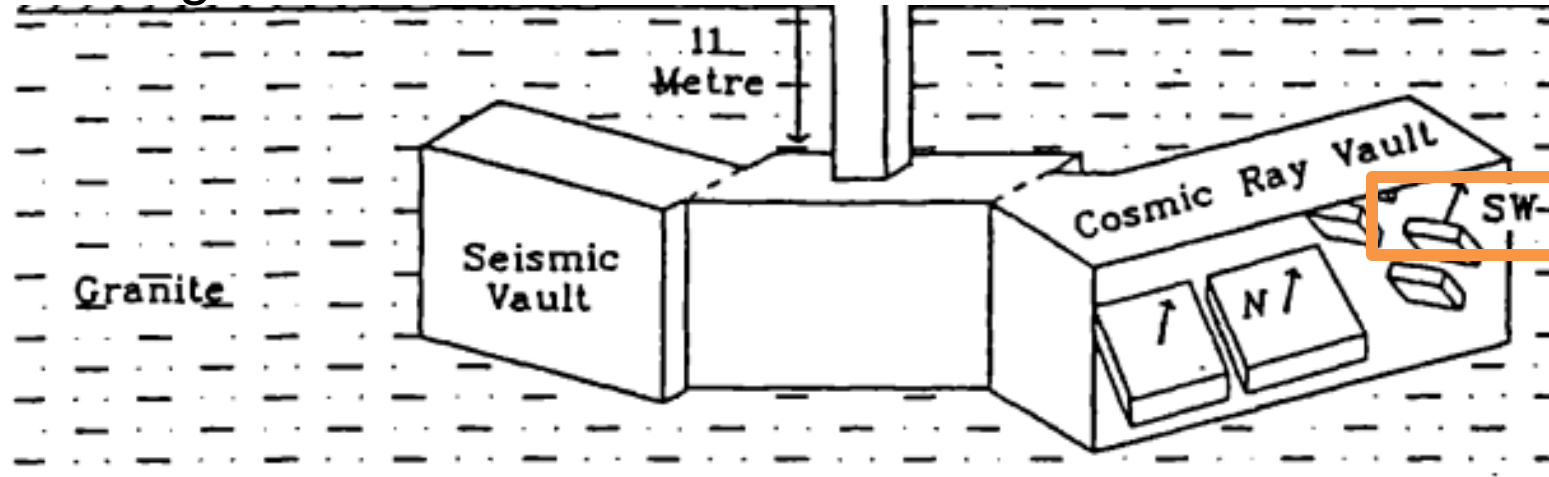
Hour data P6



Hour data P7



Underground Level

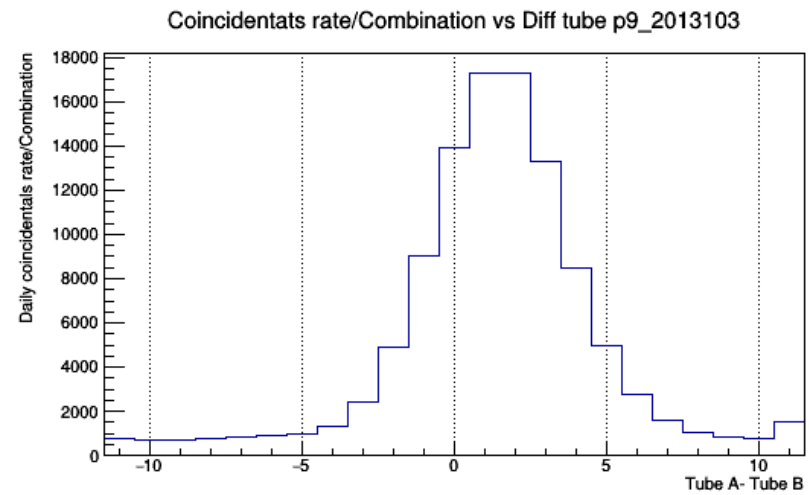
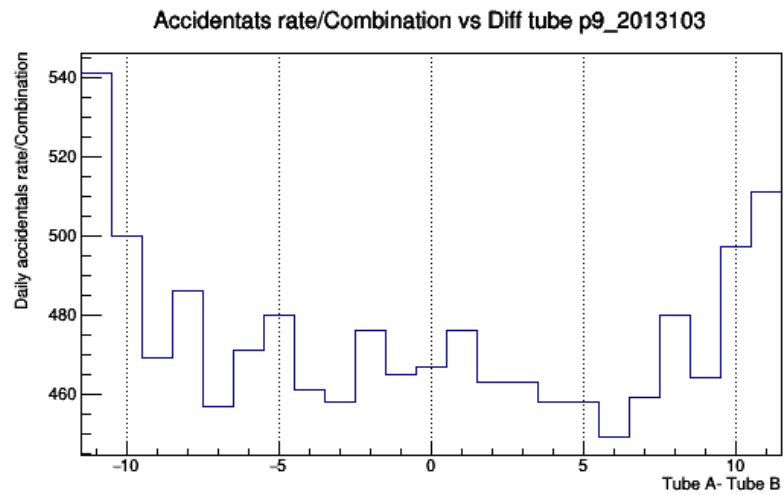
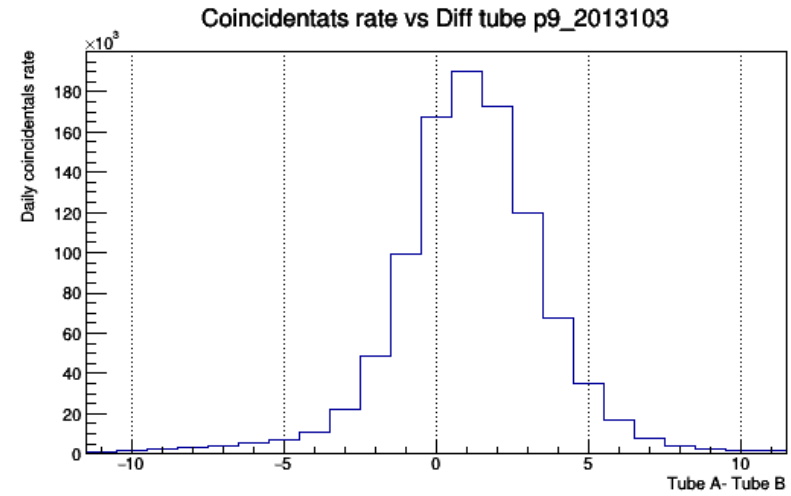
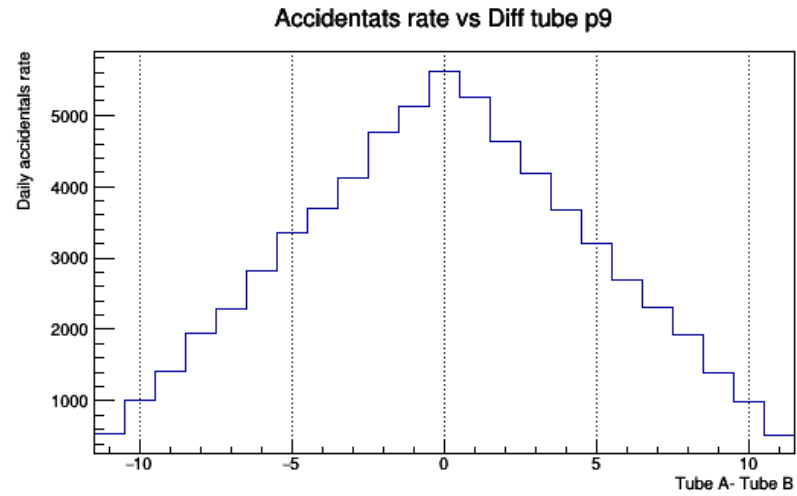


- P9 & 10 view approximately along the southern polar rotation axis after geomagnetic bending, therefore measuring the isotropic intensity. Effective mean Rig 190 GV resulting from 53 mwe granite absorber along the central viewing direction.

Manson Muon zenith
angle

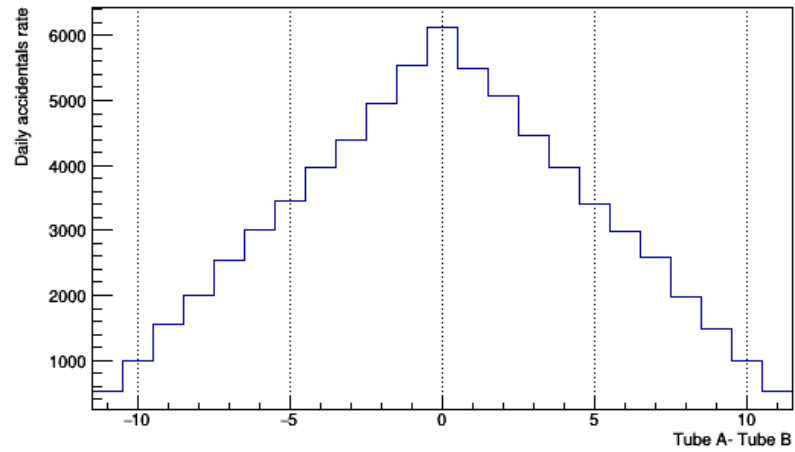
P9 & 10

P9

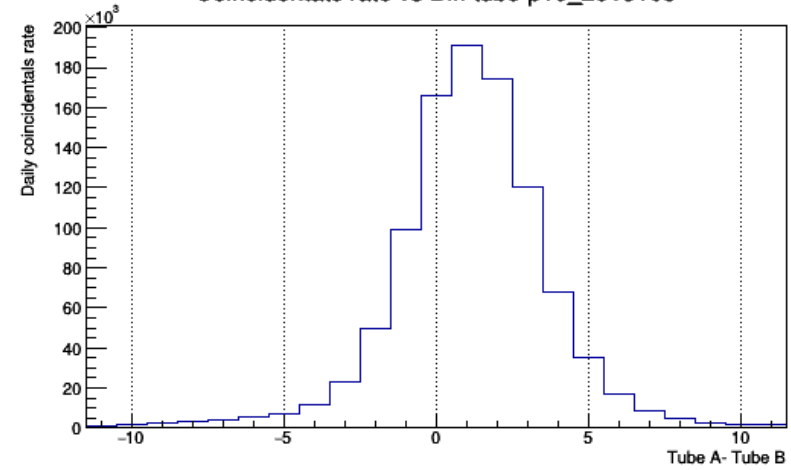


P10

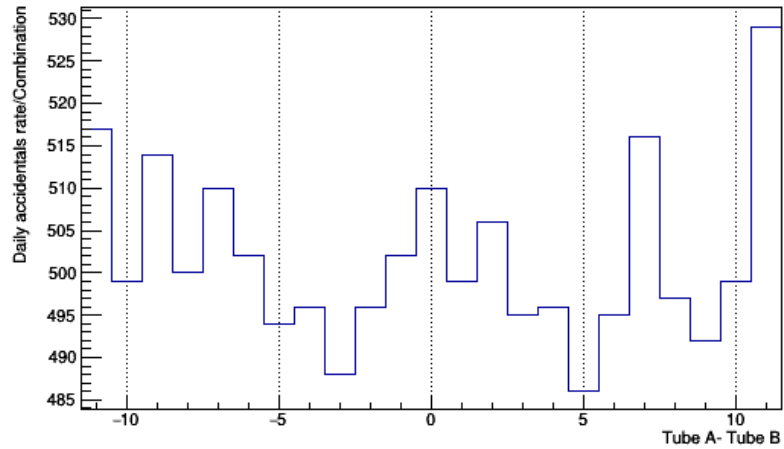
Accidentats rate vs Diff tube p10



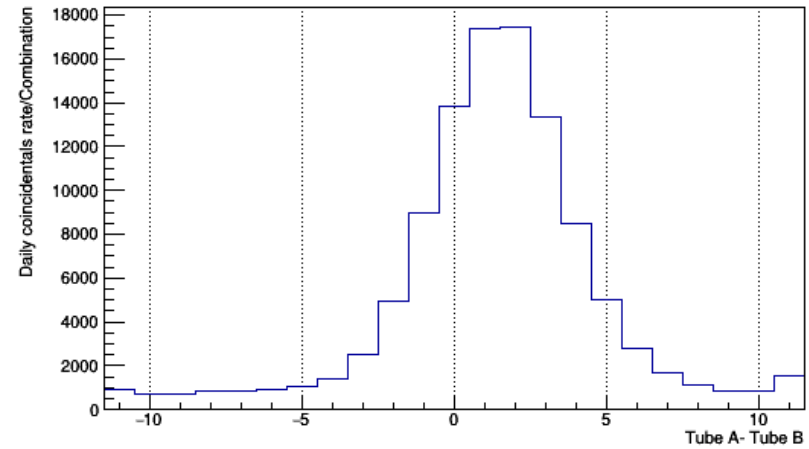
Coincidentats rate vs Diff tube p10_2013103



Accidentats rate/Combination vs Diff tube p10_2013103

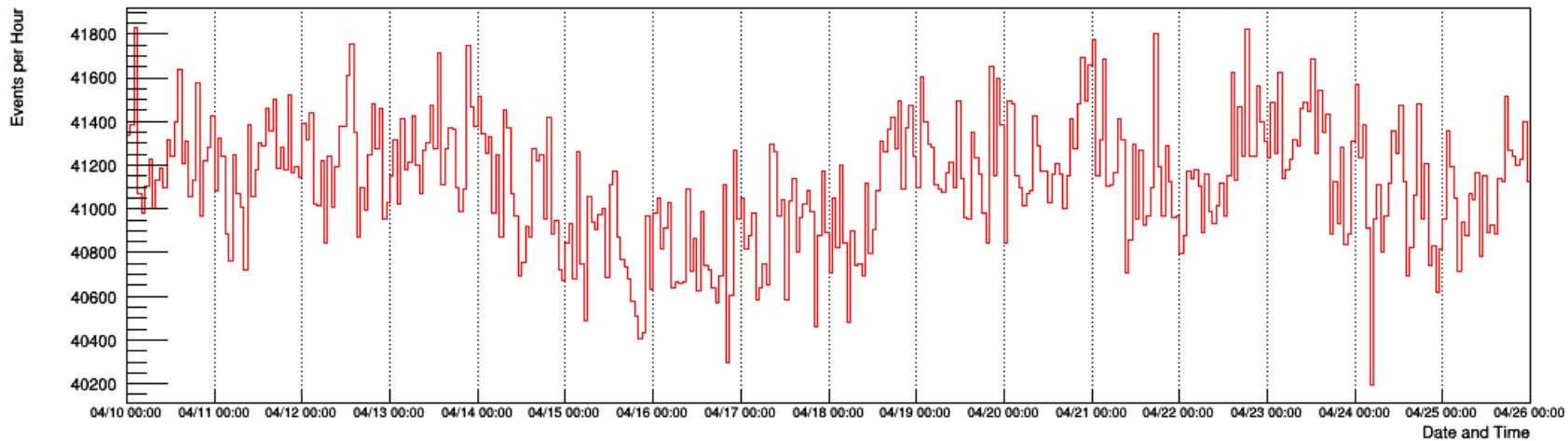


Coincidentats rate/Combination vs Diff tube p10_2013103

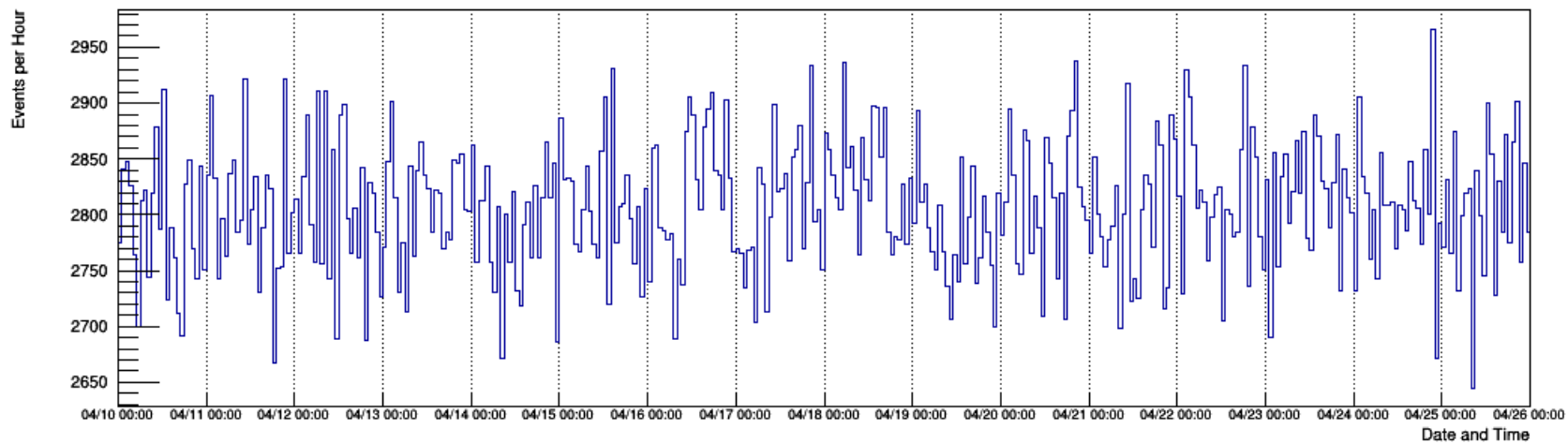


Hour data P9

p9, Hour Coincidental Rate vs Time 2013

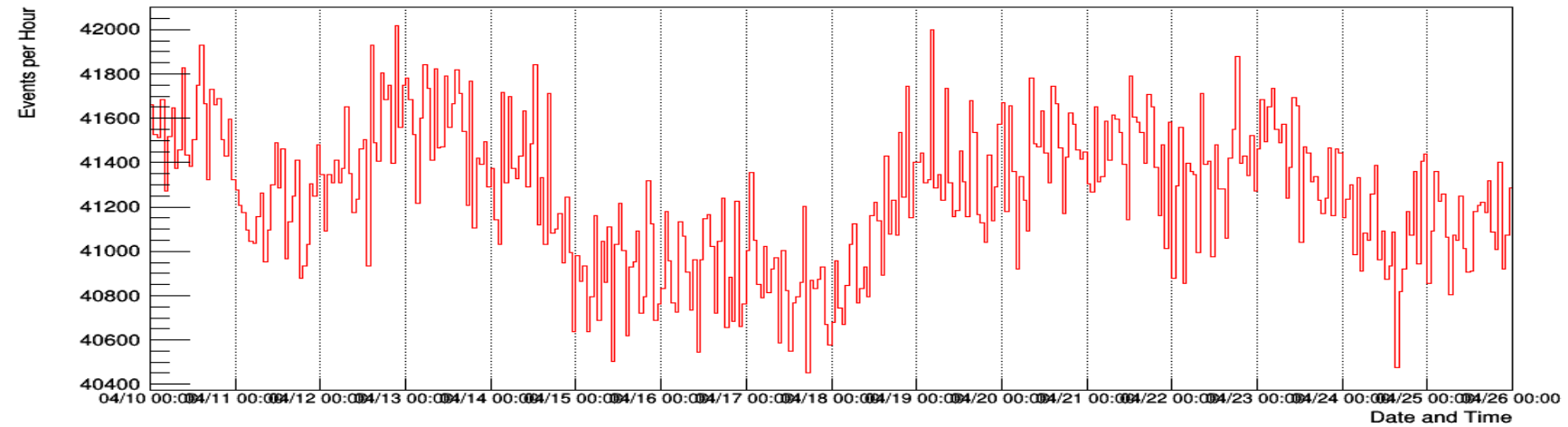


p9, Hour Accidental Rate vs Time 2013

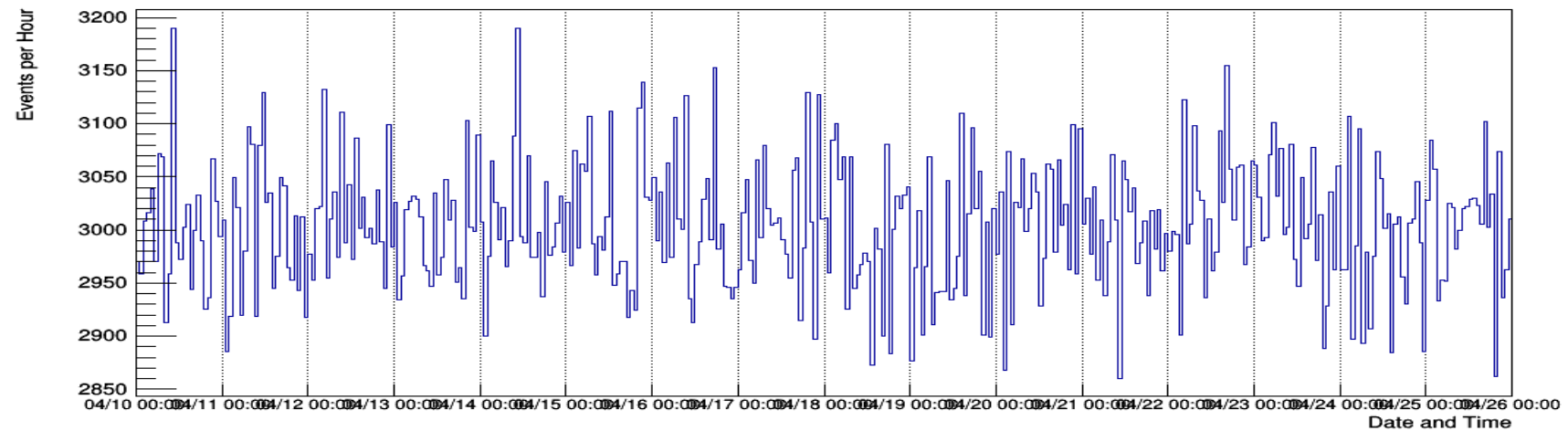


Hour data P10

p10, Hour Coincidental Rate vs Time 2013

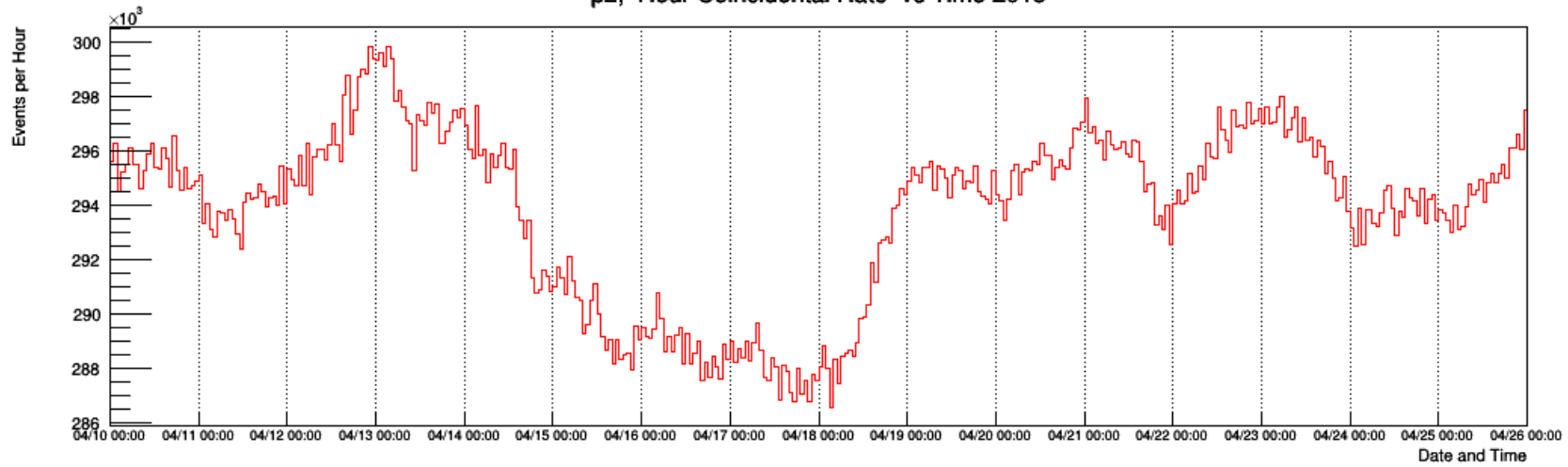


p10, Hour Accidental Rate vs Time 2013

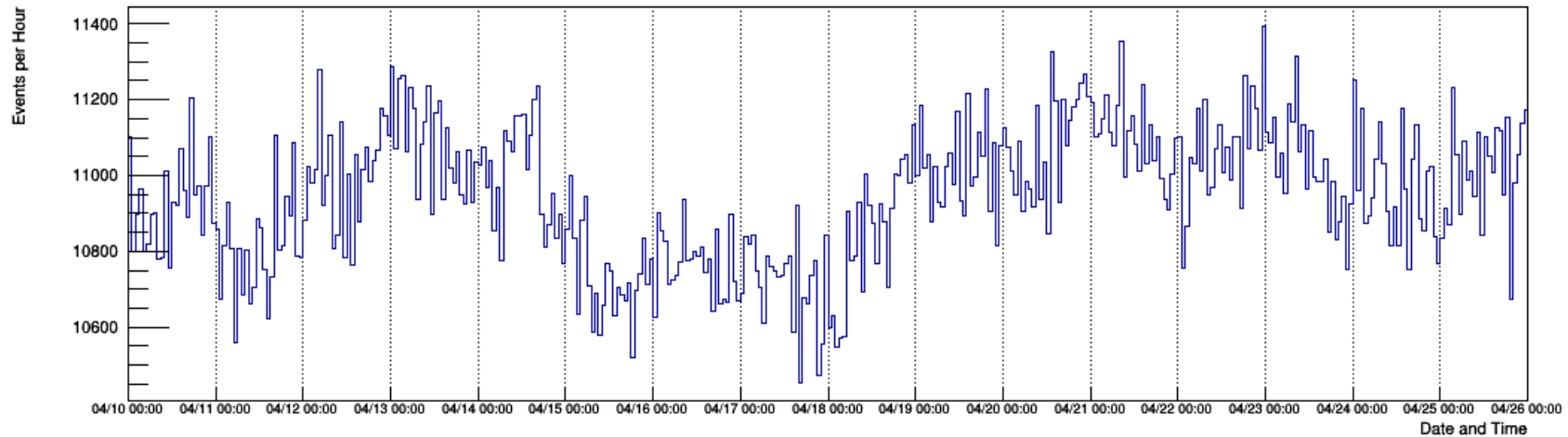


Hour data

p2, Hour Coincidental Rate vs Time 2013



p2, Hour Accidental Rate vs Time 2013





THANK YOU

ANY QUESTIONS ?

REFERENCE

Duldig, L. M. (1990). The Mawson Automatic Cosmic Ray Observatory (MACRO). In *International Cosmic Ray Conference*, volume 7 of *International Cosmic Ray Conference*, page 288.

Forbush, S. E. (1937). On the Effects in Cosmic-Ray Intensity Observed During the Recent Magnetic Storm. *Physical Review*, 51(12):1108–1109

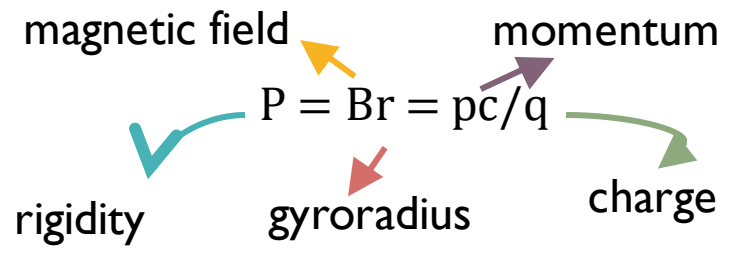
Mavromichalaki, H., Plainaki, C., Gerontidou, M., Sarlanis, C., Souvatzoglou, G., & Mariatos, G. et al. (2007). GLEs as a Warning Tool for Radiation Effects on Electronics and Systems: A New Alert System Based on Real-Time Neutron Monitors. *IEEE Transactions On Nuclear Science*, 54(4), 1082-1088.

Moraal, H., Potgieter, M. S., Stoker, P. H., and van der Walt, A. J. (1989). Neutron monitor latitude survey of cosmic ray intensity during the 1986/1987 solar minimum. *Journal of Geophysical Research: Space Physics*, 94(A2):1459–1464.

Nuntiyakul, W., Evenson, P., Ruffolo, D., Sáiz, A., Bieber, J. W., Clem, J., Pyle, R., Duldig, M. L., and Humble, J. E. (2014). Latitude Survey Investigation of Galactic Cosmic Ray Solar Modulation during 1994-2007. *The Astrophysics Journal*, 795(1):11.

GEOMAGNETIC CUTOFF RIGIDITY

➤ **Rigidity** is defined as momentum per unit charge



➤ The magnetic field of the Earth excludes particle below a well-defined rigidity at any given location known as **cutoff rigidity**

VERTICAL CUTOFF RIGIDITIES (GV)
2000 IGRF

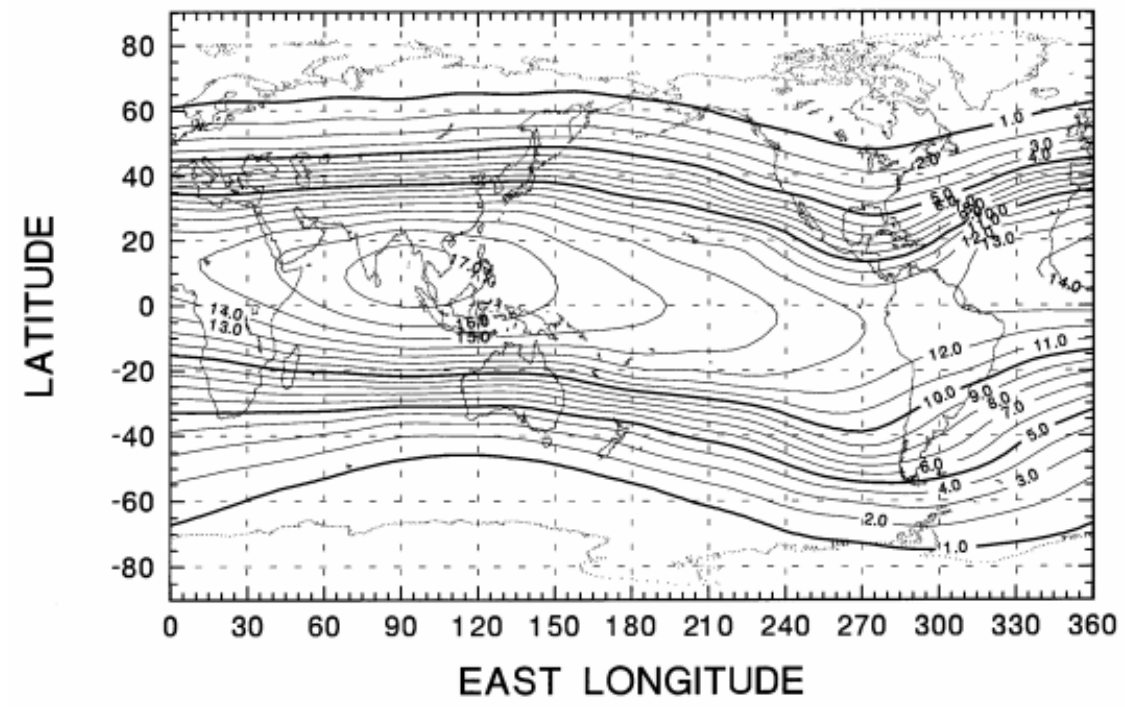


Fig 7. Rigidity contours for vertical geomagnetic cutoff rigidities for epoch 2000. (Smart & Shea, 2006)

Vertical cutoff rigidity
→ the minimum rigidity for a vertical incident particle

Apparent cutoff rigidity
→ an estimate rigidity for each possible direction of incident particle

CUTOFF-RIGIDITY

- $R_c = [M \cos \lambda^4] / \{r^2 [1 + (1 - \sin \epsilon \sin \xi \cos \lambda^3)^{1/2}]^2\}$

Where

- R_c is the geomagnetic cutoff rigidity
- λ is the latitude
- M is the magnitude of the dipole moment
- r is the distance from the dipole center in centimeters

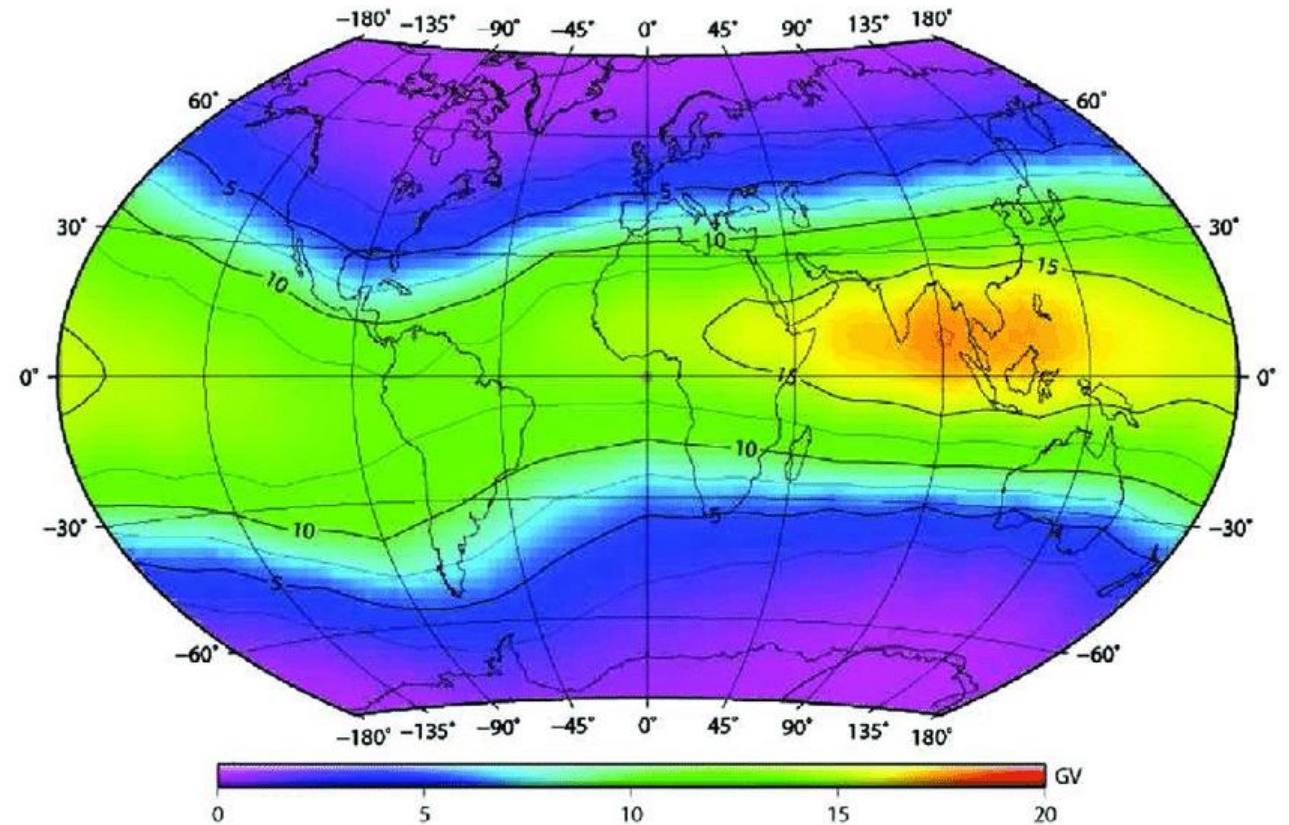


Fig 11. The effective vertical geomagnetic cutoff-rigidity (Nevalainen, Usoskin & Mishev, 2013)

NM64 RESPONSE ENERGY

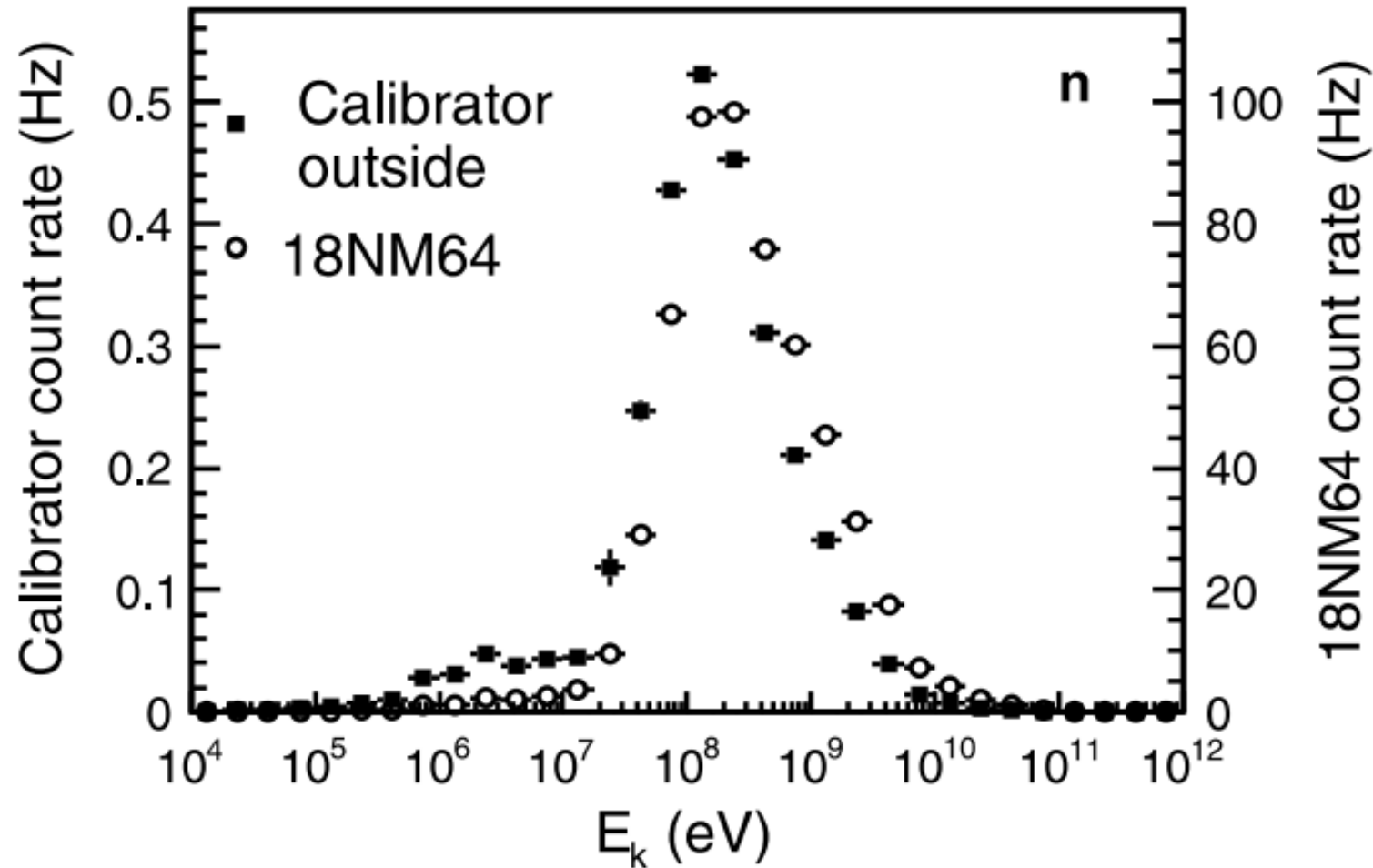


Fig 13
Simulated neutron monitor count rates produced by various types of atmospheric secondary cosmic rays arriving to ground level (Aiemsa-ad et al., 2015)

DIFFERENTIAL RESPONSE FUNCTION

$$N(P_c) = N_0(1 - e^{-\alpha P_c^{-\kappa}}),$$

$$N(P_c) = \int_{P_c}^{\infty} DRF(P) dP,$$

$$DRF(P) = N_0 \alpha P^{-\kappa-1} \kappa e^{-\alpha P^{-\kappa}}.$$

$$DRF(P) = - \left[\frac{dN}{dP_c} \right]_p \\ = \sum G(P) M(P, t) Y(P, h)$$

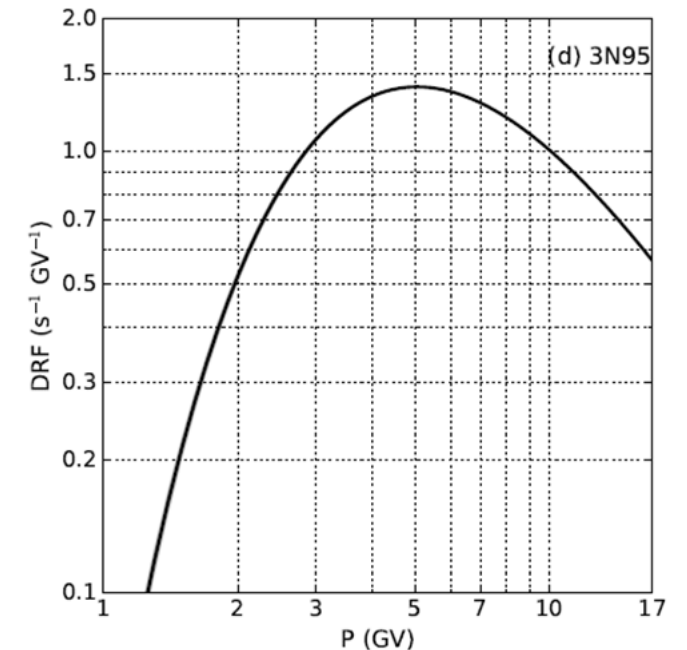
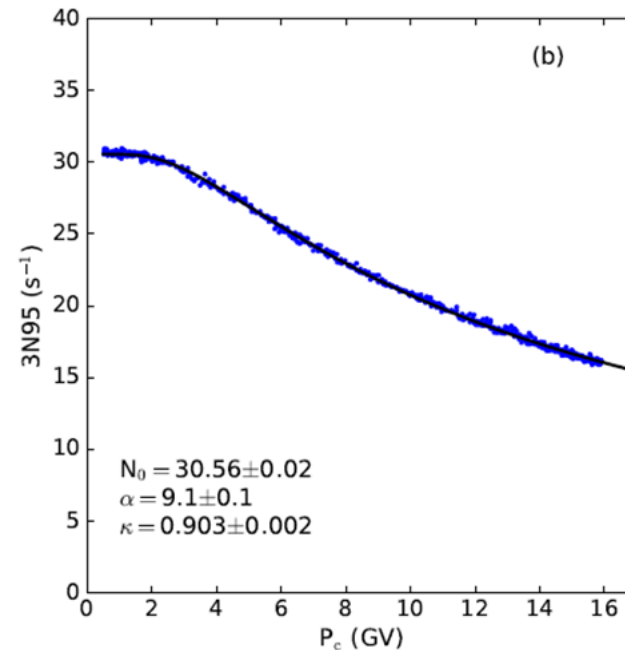
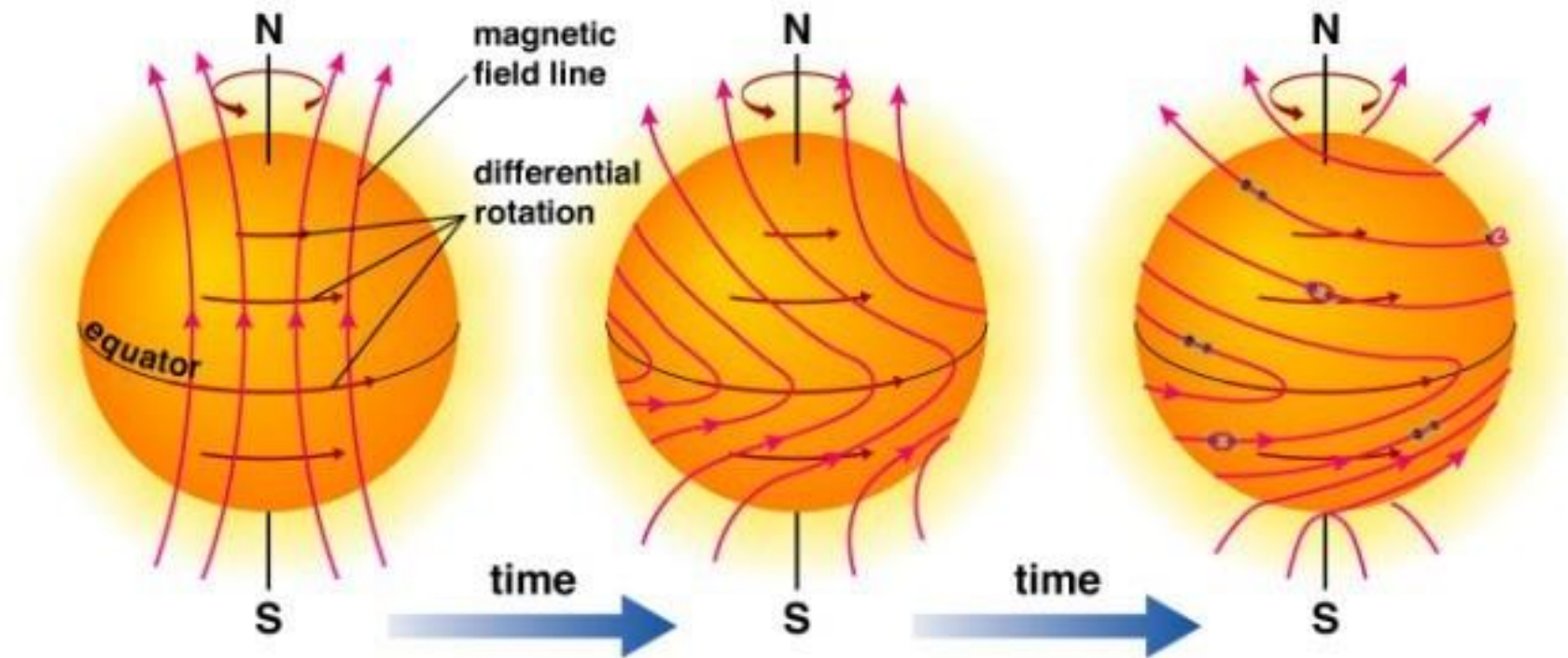


Fig 12 Dorman function fits to neutron monitor data (b) and show the resulting differential response functions (DRFs) (d) (Nuntiyakul et al., 2018)

WHAT CAUSES THE SUN'S MAGNETIC FIELD FLIP?



DATA REDUCTION

I : Tube ratio cleaning

➤ If one tube was removed

-> tube I, corrected count = $\left(\frac{s_1+s_2+s_3}{s_2+s_3}\right) (D_2 + D_3)$

➤ If two tubes were removed

-> remaining actual count rate x average ratio of whole survey

-> Only Tube I remaining, corrected count Tube 2 = $\left(\frac{D_1}{s_1/s_2}\right)$

, corrected count Tube 3 = $\left(\frac{D_1}{s_1/s_3}\right)$

➤ If three tubes were removed -> DATA GAP

DOY	T1	T2	T3	T1/T2	T2/T3	T3/T1
307.0104	8.35	9.25	8.28	0.902703	1.117150	0.991617
307.0316	8.54	9.41	8.4	0.907545	1.120238	0.983607
307.0528	8.47	9.36	8.44	0.904915	1.109005	0.996458

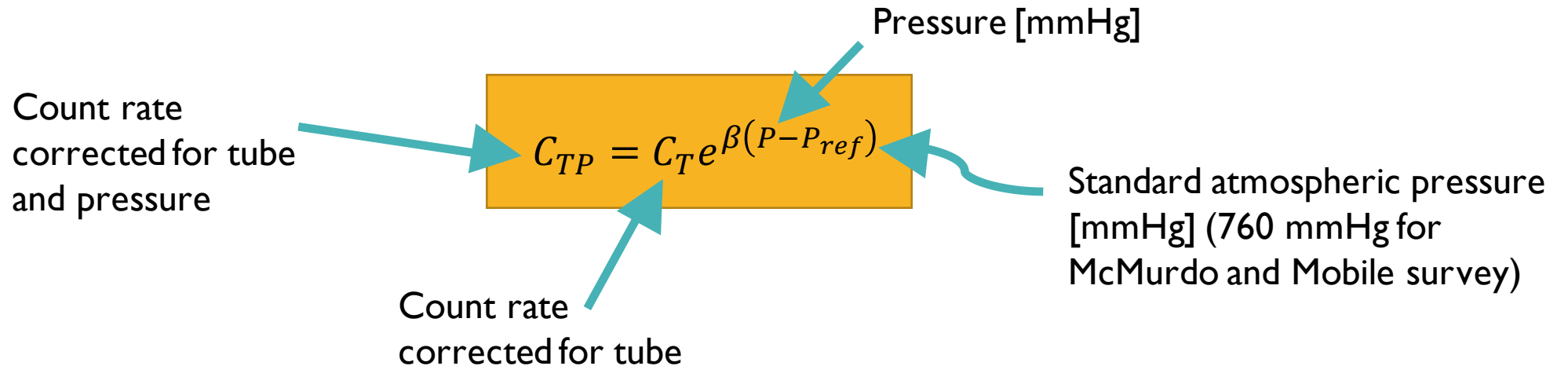
Average whole survey

↓
↓
↓
S1/S2
S2/S3
S3/S1

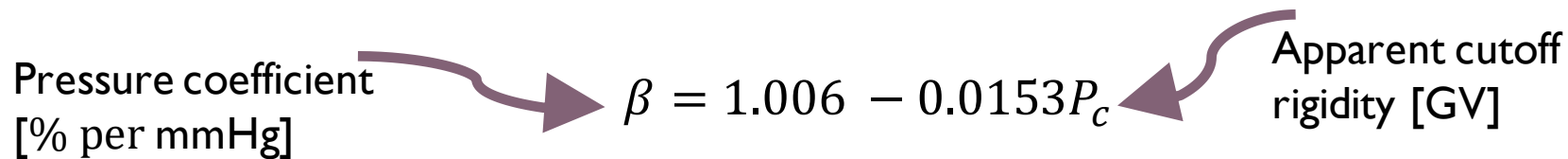
**Applied for
Mobile NM
And Mawson
NM data since
Oct 2002 to
Dec 2002**

II : Pressure correction

Barometric pressure was corrected using Equation as follow;



For latitude survey

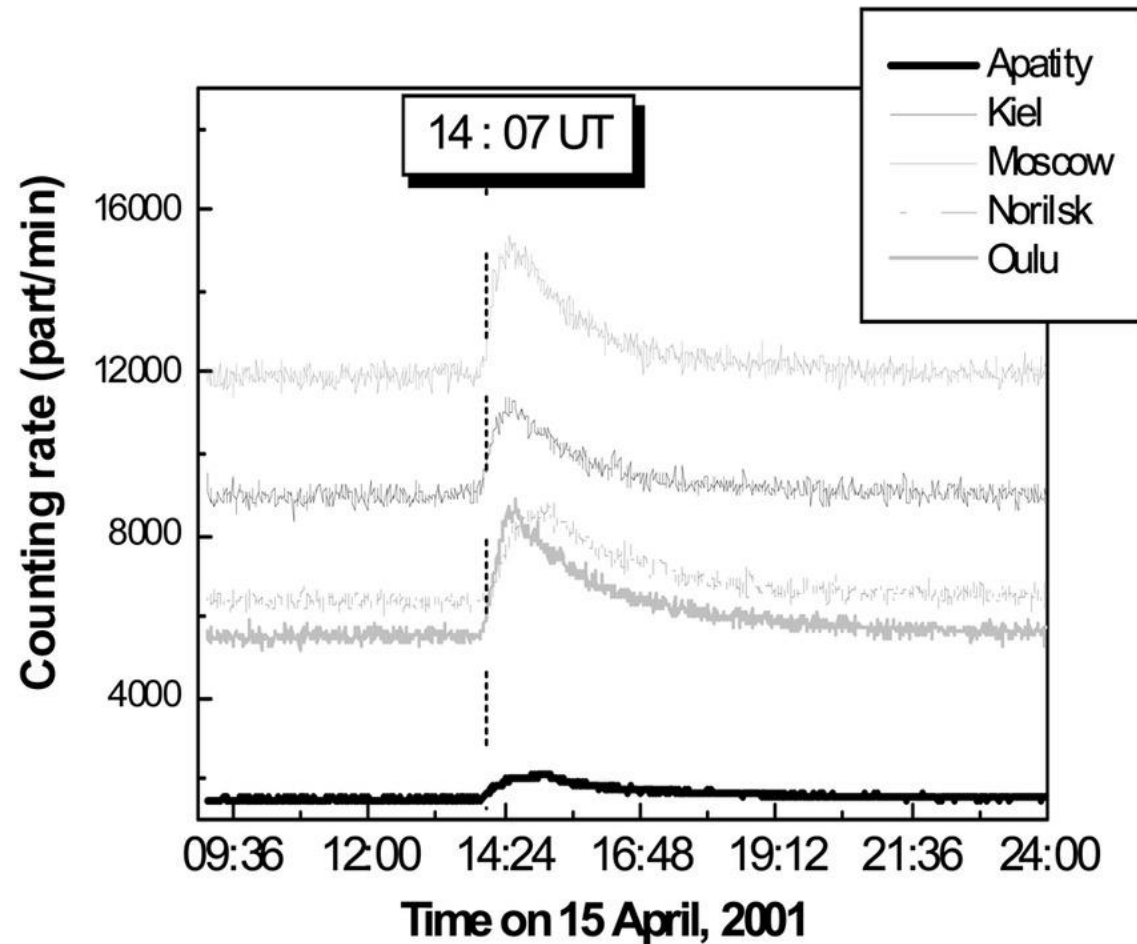


Mawson station

Standard atmospheric pressure: 990.0 mb
Barometric coefficient (2004): -0.708%/mb
* 1 mbar = 0.750062 mmHg

Applied for All data set

GROUND LEVEL ENHANCEMENT



- Ground level enhancement onsets at five NM stations recording the event of April 15, 2001 (Mavromichalaki et al., 2007)

FORBUSH DECREASE

- A rapid decrease in the observed galactic cosmic ray intensity following a coronal mass ejection (CME).

